Projections of Leaf Area Index in Earth System Models

N. Mahowald*[1], F. Lo[1], Y. Zheng[1], L. Harrison[2], C. Funk[2] ,D. Lombardozzi[3], C. Goodale[4]

[1]Department of Earth and Atmospheric Sciences, Cornell University, Ithaca, NY, 14853

[2]Department of Geography, University of California at Santa Barbara, Santa Barbara, CA 93106

[3]Climate and Global Dynamics Division, National Center for Atmospheric Research, Boulder, CO, 80307

[4]Department of Ecology and Evolutionary Biology, Cornell University, Ithaca, NY 14853

*Corresponding author: mahowald@cornell.edu

Abstract

The area of leaves in the plant canopy, measured as leaf area index (LAI), modulates key land-atmosphere interactions, including the exchange of energy, moisture, carbon dioxide (CO_2), and other trace gases and aerosols, and is therefore an essential variable in predicting terrestrial carbon, water, and energy fluxes. Here our goal is to characterize the LAI projections from the latest generation of Earth system models (ESMs) for the Representative Concentration Pathway (RCP) 8.5 and RCP4.5 scenarios. On average, the models project increases in LAI in both RCP8.5 and RCP4.5 over most of the globe, but also show decreases in some parts of the tropics. Because of projected increases in variability, there are also more frequent periods of low LAI across broad regions of the tropics. Projections of LAI changes varied greatly among models: some models project very modest changes, while others project large changes, usually increases. Modeled LAI typically increases with modeled warming in the high latitudes, but often decreases with increasing local warming in the tropics. The models with the most skill in simulating current LAI in the tropics relative to satellite observations tend to project smaller increases in LAI in the tropics in the future compared to the average of all the models. Using LAI projections to identify regions that may be vulnerable to climate change presents a slightly different picture than using precipitation projections, suggesting LAI may be an additional useful tool for understanding climate change impacts. Going forward, users of LAI projections from the CMIP5 ESMs evaluated here should be aware that model outputs do not exhibit clear-cut relationships to vegetation carbon and precipitation. Our findings underscore the need for more attention to LAI

projections, in terms of understanding the drivers of projected changes and improvements to model skill.

1.0 Introduction

Providing future projections of climate change feedbacks and impacts is one of the goals motivating the development of Earth system models (ESMs). The latest generation of ESMs includes land models that simulate the temporal evolution of carbon and vegetation (Friedlingstein et al., 2006). To do so, these models predict leaf area index (LAI) and other carbon cycle variables. LAI represents the amount of leaf area per unit land area, and is an important land carbon attribute. Many ESMs calculate leaf-level carbon and water fluxes, which are then scaled regionally and globally based on LAI (e.g. Oleson et al., 2013). The surface energy budget, as well as plant-based emissions and deposition of aerosols and chemically or radiatively important gases, are also sensitive to predicted LAI (e.g. Oleson et al., 2013). Therefore, small errors in simulated LAI can become large errors in many ESMs' biophysical and biogeochemical processes, and changes in LAI alone can change climate (e.g. Bounoua et al., 2000; Ganzeveld et al., 1998; Lawrence and Slingo, 2004; Oleson et al., 2013; Kala et al., 2014). Unlike many biophysical attributes, LAI can be observed from satellite (Zhu et al., 2013), and thus represents one of the few land carbon or vegetation variables that can be directly evaluated in coupled models (e.g. Randerson et al., 2009; Luo et al., 2012, Anav et al., 2013b). Finally changes in LAI, and the related normalized difference vegetation index (NDVI), can indicate ecosystem health and natural resource availability. As such, LAI is used within the

famine prediction community (Funk and Brown, 2006; Groten, 1993) and represents a variable that is easy to use in climate impacts studies. Thus it is important to consider the 21st century projections for LAI in Earth System Models.

The current generation of ESMs has prepared historical and future scenario simulations within the Coupled Modeling Intercomparison Project (CMIP5) (Taylor et al., 2009). There have been extensive evaluations and comparisons of the future projections of the land, ocean, and atmospheric carbon cycle in the ESMs in the CMIP5 (e.g. Arora et al., 2013a; Friedlingstein et al., 2013; Jones et al., 2013). There has also been comparison of ESM-simulated seasonal variability in LAI against satellite-based observations for the high latitudes (Anav et al., 2013a; Murray-Tortarolo et al., 2013), as well as comparisons of LAI and other variables in ESMs across the globe (Anav et al., 2013b). Additionally, Shao et al. (2013), Mao et al. (2013), and Sitch et al. (2015) evaluated the relationship between the carbon cycle and other variables, such as temperature, or LAI, over decadal and longer time scales. These ESM-based comparisons build on the long history of evaluation of model simulations of vegetation properties and carbon balance (e.g. Cramer et al., 1999).

Here, our goal is to characterize the ESM projections of future LAI in order to better understand how LAI is projected to change. Most of our analysis emphasizes the Representative Concentration Pathway (RCP) 8.5, the most extreme future scenario, and we contrast it with RCP4.5, a less extreme scenario (van Vuuren et al., 2011) (Section 3). We characterize both the model mean LAI projected change, as well as the model mean divided by the standard deviation (e.g. Meehl et al., 2007;

Tebaldi et al., 2011). In addition, we consider whether LAI projections can help the climate impact community anticipate regions that may experience increased climate exposure and increased risk of food insecurity in the future. Changes in LAI variability are also important for understanding the impact of climate change, since they can lead to an increase in the length and frequency of low LAI events, even as mean LAI increases. We consider, therefore, both changes in the mean and the frequency of low LAI events, and how this information compares to precipitation projections, which are commonly used for climate impact studies (e.g. Field et al., 2014). We also consider what model traits may be related to the spread in the future model projections (Section 3). We use evaluations of LAI, based on satellite-based observations (e.g. Zhu et al., 2013; Anav et al. 2013b; Sitch et al. 2015), to characterize the relationship between model skill and projections (e.g. Steinacher et al., 2010; Cox et al., 2013; Flato et al., 2013; Hoffman et al., 2014) (Section 4). Section 5 presents our summary and conclusions.

2.0 Methods and datasets

2.1 Model datasets

Coupled carbon model experiments were included as part of the CMIP5 experiments (e.g. Arora et al., 2013: Taylor et al., 2009). The historical simulations and Representative Concentration Pathway for 8.5 (RCP8.5; van Vuuren et al., 2011; Riahi et al., 2011), using prescribed carbon dioxide concentrations, were analyzed here (Table 1). We chose to focus on the RCP8.5 scenario as it has the largest

changes in carbon dioxide and climate. Analysis of the RCP4.5 scenario (Wise et al. 2009; van Vuuren et al., 2011) is also included for comparison for the models which included the RCP4.5 simulations at the CMIP5 archive (all models except BNU-ESM and CESM-BGC).

Model variables analyzed included monthly-mean precipitation, near surface air temperature, vegetation carbon stock and LAI. Only models which had data for all these variables for both historical and RCP8.5 scenarios were included in this study. Some models submitted multiple versions, at different resolutions or with slightly different physics (Table 1). Even though some of the models are closely related (e.g. CESM1-BGC and NorESM-ME), we include different configurations of the same model.

2.2 Model future projection analysis

This analysis examines model mean changes between the current climate (1981-2000) and future climate time periods (2011-2030, 2041-2060 and 2081-2100). To identify the location where models project statistically significant changes, we analyze the ratio of the mean change to variability; this is accomplished by dividing the mean changes over 20 year time periods by the standard deviation over the current climate (1981-2000) and shown in terms of standard deviation units (e.g. Mahlstein et al., 2012; Tebaldi et al., 2011). Previous studies have shown that the spatial and temporal scale used to define these changes can determine whether these signals are statistically significant (Lombardozzi et al. 2014). We focus on three time periods throughout the twenty-first century because the change in LAI can potentially switch between positive and negative in these different time periods

(e.g. Lombardozzi et al. 2014), and we want to identify whether the changes through time are gradual, or if there is a tipping point.

Changes in LAI variability are also important for understanding the impact of climate change. To estimate the periods of low LAI and low precipitation, we calculate the fraction of the time during which the variable is one standard deviation (evaluated in the 1981-2000 time period) below the current mean (1981-2000). By definition, if the variables have a Gaussian distribution, each gridbox would be considered having a "Low LAI" for 1/6 (16%) of the time, and this is approximately true at most grid points (not shown). We use this metric to estimate the fraction of the time in the future that this condition exists, and specifically whether it increases in the future.

2.3 Observational data

LAI data derived from satellite over the 30-year period 1981-2010 is used to evaluate the CMIP5 model skill in the current climate. This observational dataset is derived using neural network algorithms using the Global Inventory Modeling and Mapping (GIMMS) Normalized Difference Vegetation Index (NDVI3g) and the Terra Moderate Resolution Spectroradiameter (MODIS) LAI (Zhu et al., 2013). The satellite data are only available over regions with green vegetation, and thus are lacking over desert and arid regions. A detailed description of the algorithm and comparison to ground-truth observations are shown in Zhu et al. (2013). Compared with field-measured LAI, Mean Squared Errors (RMSE) in the satellite LAI estimates are estimated to be approximately 0.68 LAI, for spanning LAI ranges from < 1 to

almost 6 (Zhu et al., 2013). Comparisons with ground-based observations confirm that the new LAI product also seems to capture observed interannual variability patterns (Zhu et al., 2013).

Gridded temperature data for the period 1981-2010 were derived from the Global Historical Climatology Network and Climate Anomaly Monitoring System (GHCN_CAMS) 2m temperature dataset (Fan and Dool, 2008). Estimates of the uncertainty in temperature gridded datasets suggest that the uncertainty in temperatures at a grid box level is estimated to be between 0.2 and 1°C (Jones et al., 1997; Fan and Dool, 2008).

2.4 Methodology for evaluation of current climate LAI simulation

Several recent studies have used the same new satellite-derived LAI dataset (GIMMS LAI3g) in land model evaluation (e.g. Murray-Tortarolo et al 2013; Anav et al. 2013a; 2013b, Mao et al. 2013, Sitch et al. 2015), including some of the same land models used here. Thus we do not repeat a complete evaluation of model LAI compared to satellite LAI. We use the satellite LAI dataset to consider whether there is a relationship between the models' ability to simulate LAI in the current climate and the models' climate projections. We use a few basic metrics in this study (Table 2), which are described briefly below.

Results for the model and observations are evaluated on a 2.5°x2.5° grid based on the observed temperature data grid (see Section 2.3). For the metric analysis here, the averages shown are grid-box means, not areal averages. This allows us to use similar weighting for both the averages and the rank correlation

coefficients, and tends to weight the global analysis towards high latitudes. However, most of the analysis focuses on regional areas (tropical (<30°), mid-latitudes (>30° and <60°) and high-latitudes (>60°), where the differences between weighting by area and weighting by grid box are reduced.

We compare the satellite-based observed (LAI3g) and model-simulated mean LAI for the current climate (similar to previous studies e.g. Randerson et al., 2009; Luo et al., 2012; Anav et al., 2013b). The period 1981-2010 is used for this comparison. To examine regional differences in LAI simulations, the annual mean LAI in the models and observations are averaged and compared over different areas: global, tropical (<30°), mid-latitudes (>30° and <60°) and high-latitudes (>60°) (Table 2: mean LAI: model/obs.). A second metric evaluates the models' ability to capture spatial variations in LAI, using the spatial correlation across the grid-boxes of the annual mean LAI in the model compared to the observations (e.g. Anav et al., 2013b; Table 2: Mean: Corr.).

Important for this study is the consideration of the temporal variability simulated in the model. The magnitude of the seasonal cycle is calculated as the standard deviation of the climatological monthly means at each grid box. This metric is slightly different than how LAI has previously been evaluated in some studies (e.g. Anav et al., 2013a; Murray-Tortarolo et al. 2013; Sitch et al. 2015), but is more similar to analyses of other climate variables (Glecker et al., 2008), facilitating inclusion of LAI within climate model evaluations. Metrics for the seasonal cycle were computed using a spatial average over each region (Table 2: Std. Dev. Seasonal: Model/obs.). For the seasonal cycle, the ability to capture the timing of

phenology can be important (e.g. Anav et al., 2013a, Zhu et al., 2013). To analyze this ability, we computed the temporal correlation of observed and model-simulated monthly means at every grid box, and then averaged over each region (Table 2: Seasonal Avg. Corr.).

To evaluate the models' ability to simulate LAI interannual variability (IAV), we consider the magnitude of the interannual variability, which is calculated as the standard deviation of annual mean LAI across years at each grid box (e.g. Zhu et al., 2013). The IAV is then spatially averaged and compared between the model and satellite observations (Table 2: Std. Dev. IAV: Model/obs.). We focus our study on IAV, based on the inter-annual means, but there may be important changes in the seasonal cycle or length of growing season on an interannual time basis, which our simple approach does not consider (e.g. Murray-Tortarolo et al. 2013).

Previous studies have examined correlations between temperature and satellite- derived LAI (e.g. Anav et al., 2013a; 2013b, Zhu et al., 2013) or the closely related normalized difference vegetation index (NDVI; Zeng et al. 2013). Observed variations of LAI at high latitudes tend to be dominated by changes in temperature, while the tropics are more dominated by moisture (Anav et al., 2013a; 2013b, Zeng et al., 2013), which is also seen in coupled-carbon climate models for carbon cycle variables (e.g. Fung et al., 2005). In order to understand what may be driving the IAV in the LAI, we calculate metrics to examine the rank correlation between anomalies in LAI and anomalies in temperature and trends with time. Although correlations do not identify causation, they can help identify the strength of relationships among various driving factors.

This analysis focuses on the relationship between temperature and LAI for comparing interannual variability in the modeled and observed datasets. Sensitivity studies have indicated that the grid-box level relationship between temperature and LAI is a good indicator of features intrinsic to the model, rather than to the meteorology forcing the model (supplemental material Figure S1; as seen also in Anav et al., 2013a; Murray-Tortarolo et al., 2013). This was not the case for the relationship between precipitation and LAI. In sensitivity studies conducted as part of this study, we forced the Community Land Model (Lawrence et al., 2012; Lindsay et al., 2014), which is the land model used in the CESM (Table 1), with reanalysis derived data combined with observed precipitation (Qian et al., 2006; Harris et al., 2013) instead of model derived meteorology. The LAI-precipitation relationship across IAV was very sensitive to the meteorology used, and thus is not shown or used to evaluate the current climate simulations of LAI (supplemental material; Figure S1). This implies that errors in the simulations of the mean and variability in precipitation in the current climate, which are very difficult for ESMs to simulate well (e.g. Flato et al., 2014), are very important for the simulation of IAV in LAI.

Land use, especially the conversion from natural vegetation to agricultural use, can heavily perturb the mean and evolution of the seasonal cycle and interannual variability in current climate LAI. To determine whether this changes our model evaluation, we exclude grid boxes with more than 50% of agricultural land use based on Ramankutty et al. (2008). Results of the model evaluation with and without agricultural grid-box were quantitatively and qualitatively similar to those presented here, and thus we include all grid-boxes in this analysis. Future

simulations are unlikely to be more sensitive than the historical simulations to land use and land cover change, because the scenarios include less future land cover change than has occurred historically (Hurtt et al., 2011; Van Vuuren et al., 2011).

For ease of interpretation, we present the metrics described above in Figure 9, in which higher numbers represent a better simulation. For correlations, this representation is straightforward: 1 is a perfect correlation and lower values represent a worse simulation. For the other metrics that are not correlations, we convert the statistics to values similar ranges to facilitate ease of display. The mean model bias metric (model/obs) is normalized to a value that varies between 0 and 1, with 1 being close to the observed data. This approach penalizes models which have too high of a mean equally with model that have too low of a mean, using the following formula (Figure 9):

$$Model\ Evaluation\ Value = \frac{2}{\left\{\frac{Model\ Mean}{Observed\ Mean} + \frac{Observed\ Mean}{Model\ Mean}\right\}} \qquad (1)$$

We use this method to convert mean biases and standard deviation biases to a model evaluation value (MEV). This is a slightly different method than used in previous studies (e.g. Gleckler et al., 2008), as the MEV does not square the standard deviations. Since we use ranks and rank correlations, the difference between these methods is unlikely to be important, and allows us to use a similar ranking method for mean and standard deviation comparisons.

3.0 Results

3.1 Future projections

First we consider the model mean projections of change in LAI for RCP8.5, similar to analyses for other standard model variables, and show their evolution through the 21st century (e.g. Meehl et al., 2007). Across most of the globe, LAI is projected to increase through 2081-2100, with small decreases projected for parts of Central and South America and Southern Africa (Figure 1). The increases in LAI are largest in high latitudes, mountainous regions (e.g. Tibetan plateau) and some parts of the mid-latitudes and tropics (Figure 1; for reference, mean satellite observed LAIs in the current climate are presented in Figure S2). Notice that in this study we use projections of human land use based on the RCP8.5 or RCP4.5, and thus an important human role in future land cover change is driven by the assumptions of the scenario chosen for these studies. Generally, for all the RCPs, there is less land use and land cover change projected in the future than occurred in the past (e.g. van Vuuren et al., 2011; Ward et al., 2014).

In order to isolate the changes that are statistically significant, for each model we divided the change in LAI by the IAV standard deviation. Values over 1 are considered statistically significant (e.g. following Tebaldi et al. 2011; Mahlstein et al. 2012). Using this approach, statistically significant changes in LAI start over the high latitudes, and spread over much of the globe with time (Figure 2). By 2081-2100, the increases in LAI are 8 times as large as IAV over large parts of high latitude regions, as well as the Tibetan plateau and some desert regions, indicating large changes (Figure 2c). Part of the reason for these very large normalized LAI values is that they have low IAV in the current climate. A few isolated tropical

regions are projected to have statistically significant reductions in mean LAI, such as in Central America and the Amazon basin.

Examination of the RCP4.5 shows a similar pattern of an increase in LAI over most of the globe, although lower in magnitude, based on either the mean change in LAI, or the normalized LAI change (Figure S3a and S3b). This result suggests that the pattern of change in LAI, as seen in the literature for temperature or even to a lesser extent for precipitation, is similar across different climate change scenarios, with the magnitude dependent on the magnitude of the forcing (e.g. Mitchell, 2003; Moss et al., 2010). There is a consistent relationship between changes in LAI and temperature across the different time periods for each model; that is, most models and regions show a constant slope between changes in LAI and temperature (Figure 3). Most models even show a similar slope between LAI and temperature for the RCP4.5 as the RCP8.5 (Figure S4). Recognize that the change in temperature scales with the change in CO_2 forcing from carbon dioxide fertilization as well as other physical variables such as precipitation (e.g. Mitchell, 2003; Moss et al., 2010). This similarity in slope for each model across RCPs and time periods breaks down in the tropics for a few of the models, as some show steeper increases in LAI at warmer temperatures and others shift from LAI increases to declines as warming continues (GFDL, IPSL, MIROC and MPI models) (Figure 3b). Across the tropics, LAI is projected to increase in some regions and decrease in others, so small changes in the relative area of these changes can lead to large shifts in the regional net mean LAI change. The value of spatial correlations between the RCP4.5 and RCP8.5 mean LAI change at each gridbox for the 2081-2100 time period is 0.81, 0.70, 0.79 and

0.89, for the globe, tropics, mid-latitudes and high-latitudes, respectively (averaged across the models), showing the spatial coherence in the LAI projections between these two RCPs. Even the models with the lowest spatial correlations between the two RCPs (GFDL, IPSL, MIROC and MPI) have statistically significant correlation coefficients of 0.45 or higher in the tropics, where correlations are the lowest.

The models project a wide range of future changes in LAI (Figure 3). One model (BNU-ESM) projects a large global mean increase of over 1 m^2/m^2 by 2081-2100. For the other models, projected global mean increases in LAI amounted to 0.5 m^2/m^2 or less. Some models (inmcm4, IPSL, MIROC and MPI model versions) projected small net decreases in LAI in the tropics (Figure 3). Inter-model differences become even more apparent at the grid-box level, with very different changes in LAI projected by the different models (Figure S5). The spread in model projections is discussed further below (section 4.0) in relation to whether there is a relationship between model skill at predicting LAI in the current climate and future model projections (e.g. Steinacher et al., 2010; Flato et al., 2013; Cox et al., 2013; Hoffman et al., 2014).

3.2 Identifying regions at risk due to climate change

In addition to being important for land-atmosphere biophysical and biogeochemical interactions, LAI is also one of the few ESM model variables that is directly usable by the climate impacts community, along with temperature and precipitation. This is because LAI and the closely related variable, NDVI, are used for identification and forecasting of drought and famine (e.g Funk and Brown, 2006; Groten, 1993) as well

as a general indicator of ecosystem health (e.g. Field et al., 1998). Thus LAI projections that identify the regions that are most at risk can help guide and motivate climate adaptation by identifying emergent areas of vulnerability. The model mean view of the future projections of LAI is quite optimistic (Figure 1, 2 and 3), however, if variability also increases, some regions may experience years with lower LAI more frequently than in current climate, despite having a constant or higher mean LAI. In fact, many regions, especially in the tropics, are at risk for more Low LAI years (Figure 4). Here we define % Low LAI as the % of years when the annual average is one standard deviation below the current mean (Section 2.2). If the variability and mean stayed constant, the % Low LAI would remain at 16%. More Low LAI years are projected for large areas of the tropics and subtropics where projected increases to mean LAI are small in magnitude or negligible (Figure 1c vs 4c, for example). Model mean changes between the current climate (1981-2000) and future climate time periods indicate substantial (>2x) increases in the frequency of low LAI in important agricultural areas (South America, Australia, Southeast Asia, and parts of Southern Africa) (Figure 4). Increased risk areas in Fig. 4 also coincide, in some cases, with some of the most food insecure regions of the world (e.g. Brown and Funk, 2008; Field et al., 2014). Similar to mean changes in LAI, the %Low LAI for the RCP4.5 at 2081-2100 is similar in pattern and magnitude to that seen earlier in the century for the RCP8.5 scenarios (Figure S3c vs. Figure 4).

Next we consider whether using LAI adds information compared to precipitation, which is more traditionally used in climate change impacts assessments (e.g. Stocker et al. 2013; Field et al. 2014). General correlations

between precipitation and LAI will be discussed in the next few sections, but here we consider the spatial distribution of at-risk regions as defined by LAI or precipitation changes. To do this, we first consider the mean change in normalized precipitation (Figure 5a) and the % Low Precipitation (Figure 5b), both defined equivalently to the LAI values (Section 2.2; Figure 2c and Figure 4c, respectively) for the model simulations considered here. Broadly speaking, the changes in precipitation seem to occur in similar regions as the changes in LAI, with large increases in precipitation over the high latitudes, and decreases over the subsidence zones of the tropics, as seen previously (e.g. Meehl et al., 2007; Tebaldi et al., 2012). Note that requiring the mean change to be statistically significant is a much stricter criteria than just an increase in low LAI, and thus the area identified in the two methods is quite different (Figure 5a vs. 5b). Overlaying the regions from LAI and precipitation which are either one standard deviation below the mean on average in the models (Figure 5c) or see an increase in % Low values (Figure 5d) suggests that LAI and precipitation largely show similar areas being at risk due to climate change, but there are significant regions which do not overlap. This suggests that there is potentially additional information for climate impact studies using LAI projections than using precipitation alone (Figure 5c and 5d). One of the most noticeable differences between LAI and precipitation projections is in the Mediterranean region where precipitation is projected to decrease, but LAI is not. Conversely, LAI projections suggest that some parts of South America and southern Africa are likely to experience more stress, which are not identified using precipitation. Future

studies should consider whether the results of the LAI projections are useful for impact studies specifically in these regions.

3.3 Drivers of LAI projections

Next we consider what drives the differences in model projections for LAI, using the example of RCP8.5 at 2080-2100. Here we use different model output attributes to characterize the future projections, and focus on the following variables: temperature, precipitation, and vegetation carbon. We also characterize the relationship of carbon dioxide fertilization as simulated in the models to the model projections. Note that there are many other potential drivers of the projected LAI changes that are likely to be important, and thus our study only seeks to consider the most obvious interactions, and highlights the uncertainties in the model-specific drivers of LAI projections.

By correlating temperature and LAI projections at each grid box for each model we can look for potentially causal relationships between model projections of temperature and LAI (Figure 6). This is analogous to using a ranked correlation coefficient to summarize the scatter in RCP8.5 points in Figure 3, but at each grid box instead of the regional average. There are strong positive correlations between model simulated changes in temperature and LAI in some regions, especially in parts of the northern high latitudes (Figure 6a), suggesting that models with a projected larger warming in the high latitudes also simulate larger increases in LAI. Higher temperatures may drive higher LAI, however it is important to recall that correlation does not necessary imply causation. For example, higher LAIs could also

be driving higher temperatures through LAI influence on surface albedo and changing surface energy fluxes (e.g. Lawrence and Slingo, 2004; Kala et al. 2014). In contrast to high latitudes, there are strong negative correlations across most of the tropics and subtropics (Figure 6a).

The projected changes in precipitation are strongly correlated with projected changes in LAI across different models in many locations (Figure 6b). This is consistent with the model mean analysis (Section 3.2) that showed that for most locations changes in LAI occur in the same locations as changes in precipitation (Figure 5). The correlations seen in this analysis for RCP 8.5 are similar for the RCP4.5 (Figure S6).

Next, we examine the correlation across models between the modeled changes in vegetation carbon stocks and change in LAI between current conditions and 2081-2100 (Figure 6c). The relationship between LAI and vegetation carbon is not straightforward, and depends on the specific biophysics and biogeochemistry algorithms used in the models. Many ESMs calculate photosynthetic rates per unit leaf area; these rates are then extrapolated to canopy-level gross primary production using LAI and other variables (e.g., light, nitrogen and CO_2 availability and leaf physiological parameters) (e.g., See Bonan et al., 2011, Piao et al., 2013). The simulated increases in LAI are correlated across models with simulated increases in plant carbon stocks in many low-LAI regions, including many deserts, grasslands, and tundra ecosystems (Figure 6c). Leaves compose most or all of the aboveground plant biomass in these ecosystems (e.g., Friedlingstein et al. 1999), such that increases in LAI relate directly to increases in plant carbon stocks.

Changes in LAI correlate more poorly with simulated changes in plant carbon stocks in other regions, with small or negative correlations in many boreal, temperate, and tropical forested regions (Figure 6c). Leaves typically compose only 3-5% of aboveground plant biomass in forests (Friedlingstein et al. 1999), and closed-canopy forests can contain widely variable stocks of woody biomass that typically depend more on successional status than LAI or growth rate. Differences in the fractional composition and turnover of these leaf- and woody tissues should decouple changes in LAI from changes in carbon stocks in woody biomass. As an example, in the CLM (the land model for the CESM-BGC) CO_2 fertilization causes a larger increase to wood allocation (62%) than to leaf allocation (21%) in the Southeastern US (Lombardozzi, personal communication, 2015). Thus, the issue of how LAI responds in different models is interesting and should be considered in future studies.

Another important potential contributor to the future projections of LAI is the effectiveness of carbon fertilization in the models (e.g. Arora et al., 2013). Using the carbon dioxide fertilization factor (β-land) from the Arora et al. (2013) study we use a rank correlation to explore the importance of the carbon dioxide fertilization strength for predicting future vegetation carbon and LAI across the models. Naively, we might expect models that respond more strongly with increased carbon uptake under higher CO_2 conditions (i.e. larger β-land) to have greater vegetation carbon and LAI in the future. Globally the correlation with β-land is 0.46 for vegetation carbon and -0.21 for LAI, suggesting that while some of the differences in future vegetation carbon projections across models are due to differences in the model

simulation of CO_2 fertilization, LAI changes are not necessarily related to CO_2 fertilization. At a regional extent there are interesting differences. For tropical, mid-latitude and high latitude, regions, respectively, the β-land correlation for vegetation carbon is 0.29, 0.47 and 0.60, and for β-land and LAI these values are -0.18, -0.09 and 0.21. Thus for high latitudes, especially, the projections of LAI appear to be dependent on the way the models' simulate the carbon dioxide fertilization.

It should be noted that it is difficult to identify from the correlations whether relationships are due to modeled CO2 fertilization effect or modeled simulation of LAI in the current climate. There are only two models with a low carbon dioxide fertilization effect (CESM-BGC and NOR-ESM). For high latitudes both models simulate low LAI for present day and small increases to future LAI. Thus either, or both factors could be important. These similarities likely come from both models using the same land carbon model (Thornton et al., 2009) which includes nitrogen limitation. In the tropics the carbon dioxide fertilization is negatively correlated to future LAI changes, and only slightly correlated with vegetation carbon. The negative correlation in the tropics between LAI projections and CO_2 fertilization could be due to the smaller temperature impact on carbon cycle (γ-land from Arora et al. 2013) in the nitrogen-limited models (i.e. the β-land and γ-land are negatively correlated in Table 2 of Arora et al., 2013). These models see a strong increase in nitrogen mineralization in the tropics in a warming climate, which allows an increase in productivity in the future tropics (Thornton et al., 2009).Across these simulations, whether or not the model includes dynamic vegetation does not

significantly correlate with changes in LAI in any of the regions.

Overall, the relationship of land model characteristics and LAI is not straightforward, which argues that more analysis of the complicated interactions between the details of the land biophysics and biogeochemistry, as well as biogeography changes is required in order to better understand and improve model projections of LAI.

4.0 The relationship between model skill and future projections

There are large differences between the different models' projections of future LAI (e.g. Figure 3; Figure S5; Figure 7b). Previous studies have hypothesized that they could reduce the uncertainty in future projections by looking for relationships between model metrics and future projections of climate, and then choosing the models which best match the observations in the current climate (e.g. Cox et al., 2013;Hoffman et al., 2014) or by subsampling models for different regions by their performance (e.g. Steinacher et al., 2010). In this section we explore both approaches. In essence, we are looking for a correlation between current model performance and future projections; this correlation has been used in some studies to argue for a more accurate projection, and to reduce the uncertainty in the future projections. In many cases in climate modeling and projections, there is no correlation between model skill in current climate conditions and projections (e.g. Cook and Vizy, 2006), however in some limited cases there is a correlation between metric score and a projection, and one is able to constrain future projections (e.g. Cox et al., 2013; Steinacher et al., 2010). Here we consider whether such a case

applies. In doing this type of analysis, we are making an assumption that model skill in the current climate translates into better model projections, which may be a product of real model differences or a statistical error. The advantages and disadvantages of using this type of approach are discussed in more detail in Flato et al. (2013). Here we do not advocate that such an approach leads to a better projection, but rather simply use this approach to characterize the future model projections.

4.1 **Evaluation of model LAI**

Several recent studies have evaluated the land models in ESMs using the LAI satellite records (e.g. Anav et al. 2013a; 2013b; Mao et al. 2013; Sitch et al. 2015). Thus we do not repeat those assessments, but rather briefly summarize the results of the comparisons here.

Most models tend to overestimate the mean LAI compared to the observations (Figure 8a), and this is true at all latitudes (Figure 8a, Table S2). Several models have a large overestimates (>50% too high), including bcc-csm1, bcc-csm1-1, BNU-ESM, GFDL-ESM2G, GFDL-ESM2M, MIROC-ESM. The over-prediction relative to the satellite data tend to be larger in tropical regions for most models, but the GFDL model estimates are also larger in the high latitudes (Figure 8a, Table S2). However, the satellite derived LAIs have biases; for example, they underestimate high LAIs due to being unable to see all the leaf layers in closed canopies or with high frequency of cloud cover or overestimate LAIs in more arid regions, and thus there may also be an error in the observational dataset (see

discussion in Anav et al. 2013b; Pfeifer et al. 2014 or Forkel et al., 2015, for example).

Some models also tend to over predict the strength of the seasonal cycle (e.g. bcc-csm1, BNU-ESM, MIROC-ESM) (Figure 9b; Table S1), where the strength of the seasonal cycle is measured by the globally averaged standard deviations of the monthly mean climatology. But the region in which they over-predict the strength of the seasonal cycle differs between models. Of course, there is not a strong seasonal cycle in the tropics, where the lowest standard deviations tend to occur (Figure 8e; Table S2a). Again, because of the difficulties of retrieving accurate LAI from satellites in closed canopies, the observations may underestimate the seasonal cycle in tropical forests.

Interannual variability tends to be over-predicted in some of the models (e.g. bcc-csm1, bcc-csm1_1, BNU-ESM, CESM1-BGC, GFDL-ESM2G, GFDL-ESM2M, MIROC-ESM, MIROC-ESM_CHEM) (Figure 8c, Table S1). For this calculation, the interannual variability (IAV) is calculated as the standard deviation of the annual average across multiple years. Generally, the models do a decent job simulating the spatial variability in the annual mean LAI (Figure 8d; Table S1), with the correlations being strongest in the tropics, and weakest in the high latitudes (Figure 8d; Table S2). This is likely partly due to the strength of the LAI differences in tropics and the limitation of LAI primarily by moisture alone (with low LAI in arid regions and high LAI in tropical forests). The timing of the seasonal cycle (Figure 8e; Table S1) is less well simulated in the models, with several models not having an average statistically significant correlation (~0.5 for 95% significance for 12 month seasonal cycle) on

the global scale, or in the mid- and high latitudes (e.g. GFDL, MPI-ESM-MR on global scale, GFDL, inmcm4 and MPI-ESM-MR for various regions).

Next we explore the observed and modeled relationship between LAI and temperature, and the observed and modeled trend in LAI (e.g. Anav et al., 2013a; Anav et al., 2013b; Ichii et al., 2002; Zeng et al., 2013; Mao et al., 2013; Zhu et al., 2013). As previously shown, there are positive relationships between modeled and measured LAI and temperature in high latitudes (Figure 6a; Figure S5; e.g. Anav et al. 2013a; Ichii et al., 2002; Zeng et al. 2013; Zhu et al. 2013). In the tropics (<30°), the relationship can be positive or negative but some regions tend towards a negative relationship (Figure S5; Figure 6a). This is consistent with our understanding that many places in the tropics are close to the optimal growing temperature already, and increases may lead to reduced productivity (Lobell et al., 2011), although this also could be related to moisture stress (Fung et al., 2005). Compared to the observed correlations, most models have too strong of a negative relationship between LAI and temperature in the tropics, and too strong of a positive relationship in the high latitudes (Figure 8f, Table S2a-c). In the tropics, the BNU-ESM model has a weakly positive impact of temperature, while in the high latitudes, especially the CanESM2, HadGEM2-CC, HadGEM2-ES, MPI-ESM-MR models have a much stronger correlation than observed. The model and observations show similarly weak correlations between the temperature and LAI in the mid-latitudes.

Some regions show substantial trends over time (1981-2010) in measured LAI (Figure S7b), especially in high latitudes in the Northern Hemisphere (e.g. Zhu et al., 2013; Mao et al. 2013). This could be associated with the longer growing season

due to warming (e.g. Lucht et al., 2002; Zeng et al. 2013). It is also possible that this trend is due to CO_2 fertilization effects (e.g. Friedlingstein and Prentice, 2010). For high latitudes, we find a rank correlation of 0.58 across the models between the CO_2 fertilization factor on land for the Earth system models (called the β-land in Arora et al., 2013, as discussed above) and the average correlation of observed LAI with time, suggesting that there may be a component of carbon dioxide fertilization in the models' temporal trends. These trends are stronger in the models than the observations, which may be related to an overestimate of the fertilization effect.

With regard to LAI interannual variability correlations with temperature or time, there are also strong correlations among temperature, precipitation and time themselves (e.g. IPCC, 2007). Here we do not attempt to differentiate these signals because of the statistical complexity and the shortness of the time record. The shortness of the record considered could also lead to aliasing of the real variability, especially in regions like the Sahel that have strong decadal scale variations (e.g. Loew, 2014). The observational datasets also contain measurement noise, while the model values do not. We expect the measurement noise to reduce the correlations of LAI with the environmental variables in the observations relative to the true values, as seen compared to many models (Figure 8f). Thus, our metrics for interannual variability are likely to be more impacted by uncertainty in the observations than for the annual mean or seasonal cycle, and thus they may be less useful for evaluation of the models, although potentially interesting. For this study, we consider the IAV in the annual mean, but there may be important changes in the seasonal cycle or length of growing season on an interannual time basis, which our

simple approach does not consider (e.g. Murray-Tortarolo et al. 2013). In addition, the regional or global average of some of these correlations may be difficult to interpret, as not being statistically significant (e.g. Figure 8f), thus making the LAI IAV correlations less helpful.

Figure 9 summarizes our comparisons of the models with the observations for LAI for the different metrics in Table 2 (Tables S1, S2). In order to show both correlations and model mean biases in the same figure, we have converted the model-data comparisons into Model Evaluation Values using equation (1) in Section 2.3, where 1 is a perfect model simulation and lower values represent worse model simulations. Overall, none of the models does a perfect job, and improving simulation of LAI for all models will be important. In addition, as discussed above, some models perform better in some regions than others. In order to more easily see how the models compare, we also show the ranking of the different models in each region (Table 3). For this comparison, we exclude the magnitude and correlations in the IAV, because the observational estimates for this are more likely to be in error than for the annual mean and seasonal analysis, as discussed above. Thus our overall evaluation of LAI in the models includes the following metrics: annual mean LAI, spatial correlation of annual mean, standard deviation of seasonal cycle and temporal correlation of the seasonal cycle. In the tropics the top three models are the INMCM4, the IPSL-CM5A-LR and the IPSL-CM5B-LR. For the mid-latitudes the top models are the CanESM2, IPSL-CM5A-MR and the HADGEM2-ES. For high-latitudes the top models are the BNU-ESM, bcc-csm1 and the MIROC-ESM_CHEM (Table 3; Figure 9).

1

2 **4.2 Future projections constrained by current model performance**

3 Across broad regions, we evaluate which metrics are the most useful for potentially
4 constraining future climate projections by considering how the metric is correlated
5 with the projections (Figures 8 and 9; Tables S1; S2). We consider 4 regions: the
6 globe, tropics (latitudes<30°), mid-latitudes (latitudes between 30 and 60°), and
7 high latitudes (latitudes >60°). For the first approach, we look for the metrics that
8 have the highest correlation coefficient to constrain the future estimate of change in
9 LAI (similar to Cox et al., 2013) (Figure 10a and 10b) . Using this approach, we look
10 for the model metrics (from Table 2) which have the highest correlations with
11 future projections across the models, for each of the regions. If we choose the
12 models which do the best job with the metrics, this reduces the number of models
13 included in the projections, and may reduce model spread in projections.
14 As an example, for the globe, there are two metrics that correlate the highest
15 with future projections: the average correlation of IAV in LAI with date (i.e. the
16 trend), and the global mean LAI ratio of model to observation. This analysis
17 suggests that models with the largest relative change in LAI over the last 30 years
18 (1980-2010) will have the largest change in LAI in the future (Figure 10a). It also
19 suggests that models with higher LAI in the current climate, will have a larger
20 change in the future (Figure 10b). In Fig 10a and 10b, the observation-based
21 estimates are indicated by the gray vertical bar. Notice that the projected change in
22 LAI given by models that match best with the observations differs for different
23 metrics, and thus it does not allow us to uniquely constrain the future projections

(although it does suggest that the highest values are the least likely). There is one model with a very large change in LAI in the future (BNU-ESM). We use Spearman rank correlations instead of Pearson correlations, so that these results are largely insensitive to the removal of one model.

For both the tropical region and in the global analysis, the change with time (LAI IAV correlation with date) and the mean model/observation have the largest correlations (Figure 10c and 10d). Thus models that predict high LAIs in the current climate and/or currently have large trends with time, tend to project higher LAI changes in the future. Again, these two metrics would constrain our future projections to two different LAI values, as they grey lines intersect with the slope at different LAI changes (Figure 10c and 10d). For mid-latitudes, the highest correlation (and only statistically significant correlation) is between the model predicted change in precipitation and LAI (Figure 10e). Thus mid-latitude projections of LAI are difficult to constrain based on model metrics, but are sensitive to modeled changes in precipitation (as seen also in Figure 5). For high latitudes there are three metrics with similar correlation coefficients: the average temporal correlation in the seasonal cycle, the size of the interannual variability and the size of the seasonal cycle in LAI (Figure 10f., 10g, 10h). Unfortunately again, these three metrics suggest a different projected change in LAI when the observed value is used to identify the models that are most realistic (grey line in Figure 10f, 10g and 10h).

Overall, this analysis of multiple metrics suggests that there is no single metric available that is the most important in all circumstances for improving our estimates for the changes in LAI. Thus, deduction of a more probable future LAI

projection is not available to us in this case (as opposed to Cox et al., 2013, where only one metric is presented).

The second approach for characterizing the relationship between model simulations in the current climate and future climate projections, and potentially for reducing spread in the future projections follows the ideas of Steinacher et al. (2010). Here for each region, we chose the models that performed the best for several metrics (i.e. using the rankings in Table 3), instead of just one metric at a time (as above). For this study, we chose to use the top half of the models, based on their performance for each region (Table 3), so we include 9 models out of the available 18 models for each region. Using this approach does change the mean future projections, especially for the tropics and high latitudes (Table 4; Figure 7a vs. 7b), and does reduce the spread in the model values in the tropical region, but does not reduce the mean spread in mid-latitudes or high latitudes (Table 4; Figure 7c vs. 7d). In the tropics, the top models tend to have lower future projections of changes in LAI than the average of all the models (0.07 m^2/m^2 instead of 0.16 m^2/m^2). This is actually consistent with the analysis in Figure 10, since the models with the higher skill (close to grey line) would tend to have lower or middle values of future LAI projections (Figure 10a,b). For the mid-latitudes, there is not as much difference between using all models or the top performing models (Table 6), while for high latitudes, the top models tend to project slightly higher LAI in the future, also consistent with Figure 10 (f,g,h), where the projections from the models with more consistency with the observations tend to suggest higher LAI projections compared to including all the models.

The spatial distribution of the change in the future projections using the all models in comparison to the top models is consistent with the mean over the regions, with the largest change being seen across the tropics, with a reduction in both the mean LAI projection (Figure 7a vs. 7b) as well as the standard deviation (Figure 7c vs. 7d). The changes in mid-latitudes and high latitudes from subsampling only the top performing models are not very large in most locations (Figure 7a vs. 7b). Only in the tropics is the spread in the models reduced in the future projections (Figure 7c vs. 7d). The fraction of the time that is considered to have low LAI in the future is increased in the tropics, if we only consider the top models compared to including all models (Figure 7e vs. 7f).

Our results suggest that the better performing models tend to project lower LAIs in the future in the tropics in contrast to Cox et al. (2013), which focused on carbon-temperature relationships in the Amazon and which showed that observational constraints on the models tend to suggest less loss in carbon under higher temperatures. However these results may not be inconsistent as they consider different metrics in different regions, and LAI is not necessarily linearly related to vegetative carbon or carbon uptake in the models (see discussion in Section 3.4), suggesting that more analysis of how allocation is parameterized in the land carbon models is warranted.

Our analysis suggests that using multiple metrics does provide information that allows us in some cases (especially the tropics) to change our mean future projection, and potentially reduce the spread between models predictions. Overall, including only the top models in the tropics projects a future with a smaller increase

in mean LAI and an expansion in the regions at risk for a low LAI compared to including all models. At high latitudes, focusing on the top models tends to increase the already large increase in mean in LAI compared to including all models.

5.0 Summary and Conclusions

LAI is an important term for scaling leaf-level biogeophysical and biogeochemical processes to regional and global areas, and thus it is vital to consider its change in future projections. Here for the first time we consider LAI projections across the CMIP5 models and find that over much of the globe in the future, the models project an increase in mean LAI in the RCP8.5 scenario over the 21st century. Decreases are projected in the limited regions where there is also a projected decrease in mean precipitation; these regions are constrained primarily to the tropics. The change in LAI appears to grow with carbon dioxide and temperature increases across regions over the 21st century (Figure 3). Changes in LAI projected in the RCP4.5 are largely consistent with changes in RCP8.5, but have a reduced amplitude due to the smaller carbon dioxide and climate forcing.

For assessing climate change impacts, we propose that both mean LAI and LAI variability are important in identifying vulnerable regions in future projections. The models project an increased frequency of low LAI conditions despite higher mean LAIs, especially in the tropics (Figure 4). While much of the variability in LAI is driven by changes in precipitation, projections of lower mean LAI or Low-LAI frequency can identify a slightly different set of vulnerable regions (Figure 5), and add to the information that precipitation projections provide.

In order to characterize the model projections and evaluate whether we can potentially use model skill in the current climate to reduce the spread in the future projections (e.g. Flato et al., 2013), we conducted a brief comparison of the models to available satellite-derived LAI data (Zhu et al., 2013), similar to previous analyses (e.g. Anav et al., 2013a; 2013b; Mao et al., 2013; Sitch et al., 2015). Our results support the previous conclusions that the modeled LAI could be improved in many aspects of the mean, seasonal and interannual variability, although difficulties in the observational data may preclude definitive assessment (Figure 8).

We use two different methods for relating current model skill to model projections, and find that combining multiple metrics to choose better models (e.g similar to Steinacher et al., 2010) seems to work more robustly than simply correlating one metric against future projections (e.g. Cox et al., 2013; Hoffman et al., 2014), because the different metrics suggest different future projections (Figure 10). Overall, the top-performing models (top half of the models from Table 4) suggest smaller future increases in LAI in the tropics, and more regions with more incidences of low-LAI conditions than assessments that include all the models. This approach also reduces the spread among models in the tropics. However, using only the top models did not make a large difference in projections in the mid- and high latitudes (Figure 7). Realize, however, that it is not clear that the models that perform best in the current climate have more accurate projections, as discussed in more detail in Flato et al. (2013).

Finally, the spread among the models' projections of LAI was correlated with the models' projections of precipitation (Figure 6b, and Figure 5). Thus our

projections of LAI ultimately rest on the ability of models to project future precipitation. Unfortunately, in many regions the projected changes in precipitation are not large enough to be statistically significantly outside natural variability (e.g. Tebaldi et al., 2011) and there are discrepancies between climate model and statistical model predictions (e.g. Funk et al., 2014 vs. Tebaldi et al., 2011). In addition to precipitation affecting the future projections of LAI, increasing temperatures are likely to stress systems, even if there is additional rainfall (e.g. Lobell et al., 2011), expanding the regions at risk to increased drought (Figure 5). Because of the importance of LAI for biophysical and biogeochemical interactions, as well as the potential for LAI to be useful to the impacts community, we encourage more analysis of the drivers of LAI variability and changes in the future, as well as improvements in the model mechanisms responsible for the simulation of LAI.

Acknowledgements

We acknowledge the World Climate Research Programme's Working Group on Coupled Modelling, which is responsible for CMIP, and we thank the climate modeling groups (listed in Table 1 of this paper) for producing and making available their model output. For CMIP the U.S. Department of Energy's Program for Climate Model Diagnosis and Intercomparison provides coordinating support and led development of software infrastructure in partnership with the Global Organization for Earth System Science Portals. We acknowledge NSF-0832782 and 1049033 and assistance from C. Barrett and S. Schlunegger and the anonymous reviewers. We acknowledge the assistance of the LAI development group for making the LAI 3g

product available, and the NOAA/OAR/ESRL PSD group for making the GPCP and GHCN gridded products available online at http://www.esrl.noaa.gov/psd/.. This work was made possible, in part, by support provided by the US Agency for International Development (USAID) Agreement No. LAG---A---00---96---90016---00 through Broadening Access and Strengthening Input Market Systems Collaborative Research Support Program (BASIS AMA CRSP). All views, interpretations, recommendations, and conclusions expressed in this paper are those of the authors and not necessarily those of the supporting or cooperating institutions.

Table 1 Model simulations from the Climate Modeling Intercomparison Projection (CMIP5) included in this study. All models listed here were available for the RCP8.5 analysis, while the all models except BNU-ESM and CESM-BGC were available for the RCP4.5 analysis.

Model	Land Model	Land Resolution	N-Cycle	Dynamic Veg.	Citation
BCC-CSM1	BCC-AVIM1.0	2.8°x2.8°	N	Y	(Wu et al., 2013)
BCC-CSM1-M	BCC-AVIM1.0	1.1°x1.1°	N	Y	(Wu et al., 2013)
BNU-ESM	CoLM + BNU-DGVM	2.8°x2.8°	N	Y	(BNU-ESM, http://esg.bnu.edu.cn/BNU_ESM_webs/htmls/index.html)
CanESM2	CLASS2.7+CTEM1	2.8°x2.8°	N	N	(Arora et al., 2011)
CESM1-BGC	CLM4	0.9°x1.2°	Y	N	(Lindsay et al., 2014)
GFDL-ESM2G	LM3	2.5° x 2.5°	N	Y	(Dunne et al., 2013)
GFDL-ESM2M	LM3 (uses different physical ocean model)	2.5° x 2.5°	N	Y	(Dunne et al., 2013)
HadGEM2-CC	JULES+TRIFFID	1.9° x 1.2°	N	Y	(Collins et al., 2011)
HadGEM2-ES	JULES+TRIFFID (includes chemistry)	1.9° x 1.2°	N	Y	(Collins et al., 2011)
INM-CM4	Simple model	2° x 1.5°	N	N	(Volodin et al., 2010)
IPSL-CM5A-LR	ORCHIDEE	3.7° x1.9°	N	N	(Dufresne et al., 2013)
IPSL-CM5A-MR	ORCHIDEE	2.5° x 1.2°	N	N	(Dufresne et al., 2013)
IPSL-CM5B-LR	ORCHIDEE (improved parameterization)	3.7° x 1.9°	N	N	(Dufresne et al., 2013)
MIROC-ESM_	MATSIRO+SEIB-DGVM	2.8° x 2.8°	N	Y	(Watanabe et al., 2011)
MIROC-ESM-CHEM	MATSIRO+SEIB-DGVM (adds chemistry)	2.8° x 2.8°	N	Y	(Watanabe et al., 2011)
MPI-ESM-LR	JSBACH+BETHY	1.9° x 1.9°	N	Y	(Raddatz et al., 2007)
MPI-ESM-MR	JSBACH+BETHY (ocean model higher resolution)	1.9° x 1.9°	N	Y	(Raddatz et al., 2007)
NorESM1-ME	CLM4	2.5° x 1.9°	Y	N	(Bentsen et al., 2013)

Table 2: Table of Metrics for LAI comparisons between model and observation used in the following tables. More description of these metrics are provided in Section 2.4.

Metrics		Description
Mean	Model /obs	Ratio of mean LAI from the model and observations
	Corr.	Spatial correlation of Mean LAI
Std. Dev. Seasonal	Model /obs	Ratio of seasonal cycle strength: Ratio of standard deviation of the climatological monthly mean LAI from the model and observations
	Avg. Corr.	Avg. Corr. of the temporal evolution of the climatological seasonal cycle in the model vs. observations at each grid box
Std. Dev. IAV	Model /obs	Ratio of IAV strength: ratio of standard deviation of the annual mean LAI from the model and observations
IAV LAI vs. T	Avg. Corr.	Avg. Corr. between LAI and temperature in IAV
IAV LAI vs date	Avg. Corr.	Avg. Corr. between LAI and date in IAV

Table 3: Model ranking based on performance on mean annual and seasonal cycle metrics for each region (see description in section 2.1).

	Tropical	Midlatitude	High latitude
bcc-csm1	10	10	2
bcc-csm1-1	9	8	11
BNU-ESM	18	18	1
CanESM2	17	1	16
CESM1-BGC	6	11	17
GFDL-ESM2G	14	15	17
GFDL-ESM2M	16	17	6
HadGEM2-CC	10	5	7
HadGEM2-ES	14	3	11
inmcm4	1	8	13
IPSL-CM5A-LR	2	5	13
IPSL-CM5A-MR	4	1	9
IPSL-CM5B-LR	3	4	5
MIROC-ESM	12	15	4
MIROC-ESM_CHEM-	13	14	2
MPI-ESM-LR	5	7	9
MPI-ESM-MR	7	12	15
NorESM1-ME	8	13	7

Table 4: Mean and standard deviation across models for future projections (LAI change in m^2/m^2) (2081-2100) for all models and for the top half of the models

	Tropics	Mid-latitude	High-latitude
Mean Change (all models)	0.16	0.35	0.31
Mean Change (top models)	0.07	0.31	0.37
Standard Deviation across models (all models)	0.35	0.23	0.20
Standard Deviation across models (top models)	0.25	0.24	0.24

Figure captions

Figure 1: Mean of all models for the annual mean change in LAI (m^2/m^2) over time relative to current (1981-2000) for 2011-2030 (a), 2041-2060 (b) and 2081-2100 (c) for RCP8.5.

Figure 2: Mean of all models for the annual mean change in LAI over time relative to current (1981-2000), normalized by each model's current (1981-2000) standard deviation at each grid point, for 2011-2030 (a), 2041-2060 (b) and 2081-2100 (c) for RCP8.5.

Figure 3: Scatter plot of the change in annual average surface temperature (Ts C) (x-axis) against the change in annual average LAI (m2/m2) (y-axis) for the global (a), tropics (b), mid-latitudes (c) and high-latitudes (d). Averages over four time periods are shown: 1981-2000(with 0 changes), 2011-2030, 2041-2060 and 2081-2100, connected by a line. The final point (2081-2100) for RCP8.5 is a triangle. The temperatures increase in all simulations with time, so increases in the x-axis indicate an increase in time. Note that there are 4 points along each line, and thus if there is no inflection point, the slope of the line is constant across the 21st century. A similar plot including RCP4.5 is included in Figure S4.

Figure 4: Mean of the models for the fraction of the time during which the annual mean LAI is considered "Low" (model projected annual mean LAI is less than one standard deviation of the current mean at each gridbox) is shown for 2011-2030 (a),

2041-2060 (b) and 2081-2100 (c) for RCP85, where the current mean and standard deviation are defined for each grid box for 1981-2000. For the current climate, the fraction of time below one standard deviation will be 0.16, which is colored in grey, so all colors represent an increase in low LAI.

Figure 5: Mean of all models for the change in annual mean precipitation for 2081-2100 compared to current (1981-2000), normalized by the model standard deviation for RCP8.5 (similar to Figure 2c, but for precipitation) (a). Mean of the models % of the time during which the annual mean precipitation is one standard deviation below current values (similar to figure 5c, but for precipitation) for 2081-2100 in RCP8.5 (b). Grid-boxes identified as statistically significantly decreasing in LAI (green) or precipitation (blue) or both (red) (i.e. the blue regions in Figure 2a and Figure 6a contrasted) (c). Grid-boxes identified as having an increase in the amount of time with Low LAI (green) or precipitation (blue) or both (red) (i.e. the blue regions in Figure 5c and Figure 6b contrasted) (c).

Figure 6: Rank correlation across models at every grid box of the mean model change in LAI (2081-2100 minus 1981-2000) for RCP8.5 against the model change over the same time period of temperature (a), precipitation (b) and vegetation carbon stock (c).

Figure 7: Mean of all models for the annual mean change in LAI over time (2081-2100) relative to current (1981-2000), normalized by each model's current (1981-2000) standard deviation at each grid point (a) for all models (same as Figure 1c) and (b) for the top models, defined as the models performing in the top half (Table 4) for each region, tropical, mid-latitude or high-latitude. Because different models are included in different regions, there can be discontinuities at the boundaries in Figure 8b (e.g. 30 and 60 degrees latitude). The standard deviation in the mean future projection at 2081-2100 across the models at each grid point are shown for (c) all models and (d) top models. Indication of "Low" LAI is the model mean fraction of the time that LAI is more than one standard deviation below the current mean LAI and is shown for (e) all models (same as figure 5c) and (f), top models for the period 2081-2100, where the current mean and standard deviation are defined for each grid box for 1981-2000. For the current climate, the fraction of the time below one standard deviation will be 0.16, which is colored in grey, so all colors represent an increase in drought.

Figure 8: Comparison of model metrics for the LAI comparisons from Table 2 across the models, for each region (global, tropical, mid-latitude and high latitude) for a) Mean model/observations, b) seasonal std deviation model/observations, c) IAV standard deviation model/observations, d) spatial correlation of model to observed LAI, e) average temporal correlation for seasonal variability, f) average IAV LAI correlation with temperature (* indicates observed value), g) average IAV LAI correlation with time (* indicates observed value).

Figure 9: Comparison of model metrics for the annual mean and seasonal metrics from Table 2 across the models for a. global, b. tropical, c. mid-latitude and d. high-latitude regions. Similar information is shown in Table S1 and S2, but here converted to the Model Evaluation Value (equation 1) so that 1 is a perfect model simulation and lower values indicate worse simulations. Models are shown in Table 1, and listed in the figure. Metrics are mean annual (+), spatial correlation of mean annual (*), seasonal cycle standard deviation(diamond), mean seasonal cycle correlation (triangle) and interannual variability (IAV) standard deviation (square).

Figure 10: Scatterplot of the metrics with the highest absolute value of the correlation between the metric and future LAI changes across the globe (LAI IAV correlated with date (a) and mean LAI model/obs (b)) tropics (<30°) (LAI IAV correlated with date (c) and mean LAI model/obs (d)), mid-latitudes (between 30° and 50°) projected change in precipitation (e)) and high-latitudes (>50°) (seasonal cycle average correlation (f), strength of IAV model/obs (g), and seasonal cycle strength model/obs (h). The symbols are in the shown colors for each model. The grey represents the value an ideal model would have based on the observations. The black line is the line that results from a linear regression of the x and y-axis.

Bibliography

Anav, A., Murray-Tortarolo, G., Friedlingstein, P., Stich, S., Piao, S., and Zhu, Z.: Evaluation of Land Surface Models in Reproducing Satellite Derived Leaf Area Index over the High Latitude-Northern Hemisphere. Part II: Earth System Models, Remote Sensing, 5, 3637-3661, 2013a.

Anav, A., P. Friedlingstein, M. Kidston, L. Bopp, P. Ciais, P. Cox, C. Jones, M. Jung, R. Myneni, and Z. Zhu, Evaluating the land and ocean components of the global carbon cycle in the CMIP5 earth system models, *Journal of Climate*, *26*, 6801-6843, 2013b

Arora, V. K., Boer, G. J., Friedlingstein, P., Eby, M., Jones, C., Christian, J., Bonan, G., Bopp, L., Brovkin, V., Cadule, P., Hajima, T., Ilyina, T., Lindsay, K., Tjiputra, J. F., and Wu, T.: Carbon-Concentration and carbon-climate feedbacks in CMIP5 earth system models, Journal of Climate, 26, 5289-5314, 2013.

Arora, V. K., Scinocca, J., Boer, G. J., Christian, J., Denman, K. L., Flato, G., Kharin, V., Lee, W., and Merryfield, W.: Carbon emission limits required to satisfy future representative concentration pathways of greenhouse gases, Geophysical Research Letters, 38, L05805, doi:10.1029/2010GL046270, 2011.

Bentsen, M., Bethke, I., Debernard, J., Iversen, T., Kirkevag, A., Seland, Ø., Drange, H., Roelandt, C., Seierstad, I., Hoose, C., and Kristjansson, J.: The Norwegian Earth System Model, NorESM1-M- Part 1: Description and basic evaluation of the physical climate, Geoscientific Model Development, 6, 687-720, 2013.

Bonan, G., P. Lawrence, K. Oleson, S. Levis, M. Jung, M. Reichstein, D. LAwrence, and S. Swenson, Improving canopy processes in the Community Land Model version 4 (CLM4) using global flux fields empirically inferred from FLUXNET data, *Journal of Geophysical Research*, *116*(G02014), doi:10.1029/2010JG001593, 2011

Bounoua, L., Collatz, G., Los, S. O., Sellers, P., Dazlich, D., Tucker, C., and Randall, D.: Sensitivty of climate to changes in NDVI, Journal of Climate, 13, 2277-2292, 2000.

Collins, W. J., Bellouin, N., Doutriaux-Boucher, M., Gedney, N., Halloran, P., Hinton, T., Hughes, J., Jones, C., Joshi, M., Liddicoat, S., Martin, G., O'Connor, F., Rae, J. G., Senior, C., Stitch, S., Totterdell, I., Wiltshire, A., and Woodward, S.: Development and evaluation of an Earth-system model--HadGEM2, Geoscientific Model Development, 4, 997-1062; doi:1010.5194/gmdd-1064-1997-2011, 2011.

Cook, K. and Vizy, E.: Coupled model simulations of the West African Monsoon System: Twentieth- and Twenty-First-Century Simulations, Journal of Climate, 19, 3681-3703, 2006.

Cox, P., Pearson, D., Booth, B., Friedlingstein, P., Huntingford, C., Jones, C., and Luke, C.: Sensitivity of tropical carbon to climate change constrained by carbon dioxide variability, Nature, 494, 341-344, 2013.

Cramer, W., Kicklighter, D. W., Bondeau, A., Moore, B., Churkina, G., Nemry, B., Ruimy, A., and Schloss, A. e. a.: Comparing global models of terrresrial net primary production (NPP): overview and key results, Global Change Biology, 5, 1-15, 1999.

Doherty, R., Stich, S., Smith, B., Lewis, S., and Thornton, P.: Implications of future climate and atmospheric CO2 content for regional biogeochemistry, biogeography and ecosystem services across East Africa, Global Change Biology, 16, 617-640; doi:610.1111/j.1365-2486.2009.01997.x, 2010.

Dufresne, J.-L., Foujols, M.-A., Denvil, S., Caubel, A., Marti, O., Aumont, O., Balkanski, Y., Bekki, S., Bellenger, H., Benshila, R., Bony, S., Bopp, L., Braconnot, P., Brockmann, P., Cadule, P., Cheruy, F., Codron, F., Cozic, A., Cugnet, D., de Noblet, N., Duvel, J.-P., Ethe', C., Fairhead, L., Fichefet, T., Flavoni, S., Freidlingstein, P., Lefebvre, M., Lefrevre, F., Levy, C., Li, Z., Lloyd, J., Lott, F., Madec, G., Mancip, M., Marchand, M., Masson, S., Merurdesoif, Y., Mignot, J., Musat, I., Parouty, S., Polcher, J., Rio, C., Schulz, M., Swingedouw, D., Szopa, S., Talandier, C., Terray, P., Viovy, N., and Vuichard, N.: Climate change projections using the IPSL-CM5 Earth system modl: From CMIP3 to CMIP5, Climate Dynamics, 40, 2123-2165, 2013.

Dunne, J., John, J., Sheviliakova, E., Stouffer, R. J., Krasting, J., Malyshev, S., Milly, P., Sentman, L., Adcroft, A., Cooke, W., Dunne, K., Harrison, M., Krasting, J., Malyshev, S., Milly, P., Phillips, P., Sentman, L., Samuels, B., Spelman, M., Winton, M., Wittenberg, A., and Zadeh, N.: GFDL's ESM2 global cupoled climate-carbon Earth system models. Part II: Carbon System formation and baseline simulation characteristics, Journal of Climate, 26, 2247-2267, 2013.

Fan, Y. and Dool, v. d.: A global monthly land surface air temperature analysis for 1948-present, Journal of Geophysical Research, 113, D01103, doi:10.1029/2007JD008470, 2008.

Field, C., Behrenfeld, M., Randerson, J., Falkowski, P., 1998. Primary Production of the Biosphere: Integrating Terrestrial and Oceanic Components. Science 281, 237; doi:210.1126/science.1181.5374.1237.

Field, C. B., et al., Technical Summary, in *Climate Change 2014: Impacts, Adaptation, and Vulnerability. Part A: Global and Sectoral Aspects. Contribution of Working Group II to the Fifth Assessment Report of the Intergovernmental Panel on Climate Change*, edited by C. B. Field, et al., pp. 35-94, Cambridge University Press, Cambridge, United Kingdom and New York, NY, USA, 2014.

Flato, G., et al., Chapter 9: Evaluation of climate models, in *Climate Change 2013: The Physical Science Basis. Contribution of Working Group I to the Fifth Assessment Report of the Intergovernmental Panel on Climate Change*, edited by T. F. Stocker, D. Qin, G.-K. Plattner, M. Tignor, S.K. Allen, J. Boschung, A. Nauels, Y. Xia, V. Bex and P. M. Midgley, Cambridge University Press, Cambridge, UK and New York, NY, 2013.

Forkel, M., Carvalhais, N., Verbesselt, J., Mahecha, M., Neigh, C., and Reichstein, M.: Trend Change Detection in NDVI Time Series: Effects of Inter-annual Variability and Methodology, Remote Sensing, 5, 2113-2144:doi: 2110.3390/rs5052113, 2013.

Forkel, M., Migliavacca, M., Thonicke, K., Reichstein, M., Schaphoff, S., Weber, U., Carvalhais, N., 2015. Codominant water control on global interannual variability and trends in land surface phenology and greennes. Global Change Biology 21, 3414-3435; doi:3410.3111/gcb.12950.

Friedlingstein P, G Joel, CB Field, and IY Fung, Toward an allocation scheme for global terrestrial carbon models. Global Change Biology 5:755-770, 1999.

Friedlingstein, P., Cox, P., Betts, R., Bopp, L., Bloh, W. v., Brovkin, V., P. Cadule, Doney, S., Eby, M., I. Fung, G. Bala, J. John, C. Jones, F. Joos, T. Kato, M. Kawamiya, Knorr, W., K. Lindsay, H. D. Mathews, T. Raddatz, P. Rayner, Reick, C., E. Roeckner, Schnitzler, K.-G., Schnurr, R., K. Strassmen, A. J. Weaver, C. Yoshikawa, and Zeng, N.: Climate-carbon cycle feedback analysis, results from the C4MIP Model intercomparison, J. Climate, 19, 3337-3353, 2006.

Friedlingstein, P., Meinshausen, M., Arora, V. K., Jones, A., Anav, A., Liddicoat, S., and Knutti, R.: Uncertainties in CMIP5 climate projections due to carbon cycle feedbacks, Journal of Climate, 2013. *27*, 511–526, doi:510.1175/JCLI-D-1112-00579.00571.

Friedlingstein, P. and Prentice, I. C.: Carbon-climate feedbacks: a review of model and observation based estimates, Current Opinion in Environmental Sustainability, 2, 251-257, 2010.

Fung, I., Doney, S., Lindsay, K., and John, J.: Evolution of carbon sinks in a changing climate, Proceedings of National Academy of Science, 102, 11201-11206, 2005.

Funk, C. and Brown, M.: Intra-seasonal NDVI change projections in semi-arid Africa, Remote Sensing of Environment, 101, 249-256, 2006.

Funk, C., Hoell, A., Shukla, S., Bladé, I., Liebmann, B., Roberts, J. B., and Husak, G.: Predicting East African spring droughts using Pacific and Indian Ocean sea surface temperature indices, Hydrology and Earth System Sciences, 11, 3111-3136, 2014.

Ganzeveld, L., Lelieveld, J., and Roelofs, G.-J.: A dry deposition parameterization for sulfur oxides in a chemistry and general circulation model, J. Geophys. Res., 103, 5679–5694, 1998.

Gleckler, P., Taylor, K. E., and Doutriaux, C.: Performance metrics for climate models, Journal of Geophysical Research, 113, D06104, doi:10.1029/2007JD008972, 2008.

Groten, S.: NDVI-crop monitoring and early yield assessment of Burkino Faso, International Journal of Remote Sensing, 14, 1495-1515, 1993.

Harris, I., Jones, P., Osborn, T., and Lister, D.: Updated high-resolution grids of monthly climatic obsevations--the CRU TS3.10 dataset, International Journal of Climatology, 2013. 623-642, doi:10.1002/joc.3711.

Hawkins, E. and Sutton, R.: The potential to narrow uncertainty in regional climate predictions, Bulletin of the American Meteorological Society, 2009. 1095-1107, DOI:10.1175/2009BAMS2607.1, 2009.

Hoffman, F., Randerson, J., Arora, V. K., Bao, Q., Cadule, P., Ji, D., Jones, C., Kawamiya, M., Khatiwala, S., Lindsay, K., Obata, A., Sheviliakova, E., Six, K., Tjiputra, J. F., Volodin, E., and Wu, T.: Causes and implications of persistent atmospheric carbon dioxide biases in Earth System Models, Journal of Geophysical Research-Biogeosciences, 119, 141-162, doi:110.1002/2013JG002381, 2014.

Hurtt, G.C., Chini, L.P., Frolking, S., Betts, R.A., Feddema, J., Fischer, G., Fisk, J.P., Hibbard, K., Houghton, R.A., Janetos, A., Jones, C.D., Kindermann, G., Kinoshita,

T., Goldewijk, K.K., Riahi, K., Shevliakova, E., Smith, S., Stehfest, E., Thomson, A., Thornton, P., Vuuren, D.P.v., Wang, Y.P., 2011. Harmonization of land-use scenarios for the period 1500-2100: 600 years of global gridded annual land-use transitions, wood harvest, and resulting secondary lands. Climatic Change 109, 117-161, doi:110.1007/s10584-10011-10153-10582.

Ichii, K., Kawabata, A., and Yamaguchi, Y.: Global correlation analysis for NDVI and climatic variables and NDVI trends: 1982-1990, Int. J. Remote Sens., 23, 3873-3878, 2002.

IPCC: Summary for Policymakers. In: Climate Change 2007: The Physical Science Basis. Contribution of Working Group I to the Fourth Assessment Report of the Intergovernmental Panel on Climate Change, Solomon, S., Qin, D., Manning, M., Chen, Z., Marquis, M., Avery, K. B., Tignor, M. Miller, H. (Eds.), Cambridge University Press, Cambridge, UK and New York, NY, USA, 2007.

Jones, C., Robertson, E., Arora, V. K., Friedlingstein, P., Sheviliakova, E., Bopp, L., Brovkin, V., Hajima, T., Kato, E., Kawamiya, M., Liddicoat, S., Lindsay, K., REICK, C., Roelandt, C., Segschneider, J., and Tjiputra, J. F.: 21st Century compatible CO2 emissions and airborne fraction simulated by CMIP5 Earth System models under 4 Representative Concentration Pathways., Journal of Climate, 26, 4398-4413; doi:.4310.1175/JCLI-D-4312-00554.00551, 2013.

Jones, P., Osborn, T., and Briffa, K.: Estimating sampling errors in large-scale temperature averages, Journal of Climate, 10, 2548-2568, 1997.

Jong, R., Verbesselt, J., Zeileis, A., and Schaepman, M.: Shifts in Global Vegetation Activity Trends, Remote Sensing, 5, 1117-1133; doi: 1110.3390/rs5031117, 2013.

Kala, J., M. Decker, J.-F. Exbrayat, A. Pitman, C. Carouge, J. Evans, G. Abramowitz, and D. Mocko, Influence of Leaf Area Index prescriptions on simulations of heat, moisture and carbon fluxes, *Journal of Hydrometeorology*, *15*, 489-503, 2014.

Lawrence, D. and Slingo, J.: An annual cycle of vegetatio in a GCM. Part I: implementation and impact on evaporation, Climate Dynamics, 22, 87-105, 2004.

Lawrence, D. M., K.W. Oleson, M.G. Flanner, C.G. Fletcher, P.J. Lawrence, S. Levis, S., Swenson, C., and G.B. Bonan: The CCSM4 land simulation, 1850-2005: Assessment of surface climate and new capabilities, J. Climate, 25, 2240-2260, 2012.

Lin, S.-J., and R. B. Rood (1997), An explicit flux-form semi-Lagrangian shallow-water model on the sphere, *Quarterly Journal of the Royal Meteorological Society*, *123*, 2477-2498.

Lindsay, K., Bonan, G., Doney, S., Hofffman, F., Lawrence, D., Long, M. C., Mahowald, N., Moore, J. K., Randerson, J. T., and Thornton, P.: Preindustrial and 20th century experiments with the Earth System Model CESM1-(BGC), Journal of Climate, 27, 8981-9005, 2014.

Lobell, D., Schlenker, W., and Costa-Roberts, J.: Climate trends and global crop production since 1980, Science, 333, 616-620, 2011.

Loew, A.: Terrestrial satellite records for climate studies: how long is long enough? A test case for the Sahel, Theoretical Applied Climatology, 115, 427-440; doi: 410.1007/s00704-00013-00880-00706, 2014.

Lombardozzi, D., Bonan, G., and Nychka, D.: The emerging anthropogenic signal in the land-atmosphere carbon cycle, Nature Climate Change, 4, 796-800, DOI: 710.1038/NCLIMATE2323, 2014.

Lucht, W., Prentice, I. C., Myneni, R., Stich, S., Friedlingstein, P., Cramer, W., Bousquet, P., Buermann, W., and Smith, B.: Climate control of the high-latitude vegetation greening trend and the Pinatubo effect, Science, 296, 1687-1689, 2002.

Luo, Y. Q., , J. T. R., Abramowitz, G., Bacour, C., Blyth, E., Carvalhais, N., Ciais, P., Dalmonech, D., Fisher, J. B., Fisher, R., Friedlingstein, P., Hibbard, K., Hoffman, F., Huntzinger, D., Jones, C. D., , C. K., Lawrence, D., Li, D. J., Mahecha, M., Niu, S. L., Norby, R., Piao, S. L., Qi, X., Peylin, P., Prentice, I. C., Riley, W., Reichstein, M., Schwalm, C., Wang, Y. P., Xia, J. Y., Zaehle, S., and Zhou, X. H.: A framework for benchmarking land models, Biogeosciences, 9, 3857-3874, 2012.

Mao, J., Shin, X., Thornton, P., Hoffman, F., Zhu, Z., and Myneni, R.: Global Latitudinal-Asymetric Vegetation Growth Trends and Their Driving Mechanisms: 1982-2009, Remote Sensing, 5, 1484-1497; doi: 1410.3390/rs5031484, 2013.

Maxino, C., McAvaney, B., Pitman, A., and Perkins, S.: Ranking the AR4 climate models over the Murray-Darling Basin using simulated maximum temperature, minimum temperature and precipitation, International Journal of Climatology, 28, 1097-1112, 2008.

Meehl, G., Stocker, T., Collins, W., Frielingstein, P., Gaye, A., Gregory, J. M., Kitoh, A., Knutti, R., Murphy, J., Noda, A., Raper, S., Watterson, I., Weaver, A., and Zhao, Z.-C.: Global Climate Projections. In: Climate Change 2007: The Physical Science Basis, Contribution of Working Group I to the Fourth Assessment Report of the Intergovernmental Panel on Climate change, Solomon, S., Qin, D., Manning, M. Chen, Z., Marquis, M., Avert, K., Tignor, M., Miller, H. (Ed.), Cambridge University Press, Cambridge, UK, 2007.

Mitchell, T., Pattern scaling: an examination of the accuracy of he technique for describing future climates, *Climatic Change*, *60*, 217-242, 2003.

Moss, R., et al., The next generaiton of scenarios for climate change research and assesment, *Nature*, *463*, 747-756; doi:710.1038/nature08823, 2010.

Murray-Tortarolo, G., Anav, A., Friedlingstein, P., Stich, S., Piao, S., Zhu, Z., Poulter, B., Zaehle, S., Alhstrom, A., Lomas, M., Levis, S., Viovy, N., and Zeng, N.: Evaluation of Land Surface Models in Reproducing Satellite-Derived LAI over the High-Latitude Northern Hemisphere. Part I: Uncoupled DGVMs., Remote Sensing, 5, 4819-4838; doi:4810.3390/rs5104819, 2013.

Oleson, K., Lawrence, D., Bonan, G., Drewniak, B., Huang, M., Koven, C., Levis, S., Li, F., Riley, W., Subin, Z., Swensen, S., Thornton, P., Bozbiyik, A., Fisher, R., Kluzek, E., Lamarque, J. F., Lawrence, P., Leung, L. R., Lipscomb, W., Muszala, S., Ricciuto, D., Sacks, W., Sun, Y., Tang, J., and Yang, Z.-L.: Technical Description of version4.5 of the Community Land Model (CLM), NCAR, Boulder, CO, 2013.

Pfeifer, M., Lefebvre, V., Gonsamo, A., Pellikka, P., Marchant, R., Denu, D., and Platts, P.: Validating and linking the GIMSS Leaf Area Index (LAI3g) with Environmental Controls in Tropical Africa, Remote Sensing, 6, 1973-1990; doi: 1910.3390/rs6031973, 2014.

Qian, T., Dai, A., Trenberth, K., and Oleson, K.: Simluation of global land surface conditions from 1948 to 2004. part I: forcing data and evaluations, American Meteorological Society, 2006. 953-975, 2006.

Raddatz, T., Reick, C. H., Knorr, W., Kattge, J., Roeckner, E., Schnur, R., Schnitzler, K.-G., Wetzel, P., and Jungclaus, J.: Will the tropical land biosphere dominate the climate-carbon cycle feedback during the twenty-first century?, Climate Dynamics, 29, 565-574, 2007.

Ramankutty, N., Evan, A., Monfreda, C., and Foley, J.: Farming the planet: the geographic distribution of global agricultural lands in the year 2000, Global Biogeochemical Cycles, 22, BG1003, 10.1029/2007GB002952, 2008.

Randerson, J., Hoffman, F., Thornton, P., Mahowald, N., Lindsay, K., Lee, Y.-H., Nevison, C. D., Doney, S., Bonan, G., Stockli, R., Covey, C., Running, S., and Fung, I.: Systematic assessment of terrestrial biogeochemistry in coupled climate-carbon models, Global Change Biology, 15, 2462: doi:2410.1111/j.1365-2486.2009.01912x, 2009.

Rasch, P., D. Coleman, N. Mahowald, D. Williamson, S.-J. Lin, B. Boville, and P. Hess (2006), Characteristics of atmospheric transport using three numerical formulations for atmospheric dynamics in a single GCM framework, *Journal of Climate*, *19*, 2243-2266

Riahi, K., S. Rao, V. Krey, C. Cho, V. Chikov, G. Fischer, G. Kindermann, N. Nakicenovic, and P. Rafaj, RCP 8.5--A scenario of comparatively high greenhouse gas emissions, *Climatic Change*, *109*, 33-57; doi:10.1007/s10584-10011-10149-y, 2011.

Shao, P., Zeng, X., Sakaguchi, K., Monson, R., and Zeng, X.: Terrestrial carbon cycle: climate relations in eight CMIP5 Earth System MOdels, Journal of Climate, 26, 8744-8764, 2013.

Sitch, S., Friedlingstein, P., Gruber, N., Jones, S., Murray-Tortarolo, G., Ahlstrom, A., Doney, S., Graven, H., Heinze, C., Huntingford, C., Levis, S., Levy, P., Lomas, M., Poulter, B., Viovy, N., Zaehle, S., Zeng, N., Piao, S., LeQuere, C., Smith, B., Zhu, Z., and Myneni, R.: Recent trends and drivers of regional sources and sinks of carbon dioxide, Biogeosciences, 12, 653-679; doi: 610.5194/bg-5112-5653-2015, 2015.

Steinacher, M., Joos, F., Frolicher, T. L., Bopp, L., Cadule, P., Cocco, V., Doney, S. C., Lindsay, K., Moore, J. K., Schneider, B., and Segschneider, J.: Projected 21st century decrease in marine productivity: a multi-model analysis, Biogeosciences, 7, 979-1005, 2010.

Stocker, T., et al., Technical Summary, in *Climate Change 2013: The Physical Science Basis. Contribution of Working Group I to the Fifth Assessment Report of the Intergovernmental Panel on Climate Change*, edited by T. F. Stocker, D. Qin, G.-K. Plattner, M. Tignor, S.K. Allen, J. Boschung, A. Nauels, Y. Xia, V. Bex and P. M. Midgley, Cambridge University Press, Cambridge, United Kingdom and New York, NY, USA, 2013.

Taylor, K. E.: Summarizing multiple aspects of model performance in a single diagram, Journal of Geophysical Research, 106, 7183-7192, 2001.

Taylor, K. E., Stouffer, R. J., and Meehl, G. A.: A summary of the CMIP5 Experimental Design, available at: http://cmip-

pcmdi.llnl.gov/cmip5/docs/Taylor_CMIP5_design.pdf (last access: , April 8, 2015), 2009..

Tebaldi, C., J. Arblaster, and R. Knutti (2011), Mapping model agreement on future climate projections, *Geophysical Research Letters*, *38*(L23701), doi:10.1029/2011/GL049863.

Thornton, P., Doney, S., Lindsay, K., Moore, J. K., Mahowald, N., Randerson, J., Fung, I., Lamarque, J. F., Feddema, J., and Lee, Y.-H.: Carbon-nitrogen interactions regular climate-carbon cycle feedbacks: results from an atmosphere-ocean general circulation model, Biogeosciences-discussion, 6, 3303-3354, 2009.

van Vuuren, D. P., Edmonds, J., Kainuma, M., Riahi, K., Thomson, A., Hibbard, K., Hurtt, G., Kram, T., Krey, V., Nakicenovic, N., Smith, S., and Rose, S.: The representative concentration pathways: an overview, Climatic Change, 109, 5-31, 2011.

vanVuuren, D., Elzen, M. G. d., Lucas, P., Eickhout, B., Strengers, B., Ruijven, B. v., Wonink, S., and Houdt, R. v.: Stabilizing greenhouse gas concentrations at low levels: an assessment of reduction strategies and costs, Climatic Change, 81, 119-159; doi:110.1007/s10584-10006-19172-10589, 2007.

Volodin, E., Dianskii, N., and Gusev, A.: Simulating present day climate with the INMCM4.0 coupled model of the atmospheric and oceanic general circulations, Izv. Ocean. Atmos. Phys., 46, 414-431, 2010.

Vrieling, A., de Leeuw, J., and Said, M.: Length of Growing Period over Africa: Variability and Trends from 30 years of NDVI Time Series, Remote Sensing, 5, 982-1000: doi: 1010.3390/rs5020982, 2013.

Wang, W., Ciais, P., Nemani, R., Canadell, J., Piao, S., Stich, S., White, M., Hashimoto, H., Milesi, C., and Myneni, R.: Variations in atmospheric CO2 growth rates coupled with tropical temperature, Proceedings of the National Academy of Science USA, 110, 13061-13066; doi: 13010.11073/pnas.1219683110, 2013.

Ward, D. S., Mahowald, N., and Kloster, S.: Potential climate forcing of land use and land cover change, Atmospheric Chemistry and Physics, 14, 12701-12724, 2014.

Watanabe, S., Hajima, T., Sudo, K., Nagashima, T., Takemura, T., Okajima, H., Nozawa, T., Kawase, H., Abe, M., Yokohata, T., Ise, T., Sato, H., Kato, E., Takata, K., Emori, S., and Kamamiya, M.: MIROC-ESM 2010: Model description and basics results of CMIP5-20c3m experiments, Geoscientific Model Development, 4, 845-872, 2011.

Wise, M., K. V. Calvin, A. Thomson, L. E. Clarke, B. Bond-Lamberty, R. Sands, S. J. Smith, A. C. Janetos, and J. A. Edmonds, Implications of limiting CO2 concentrations for land use and energy, *Science*, *324*, 1183-1186, 2009.

Wu, T., Li, W., Ji, J., Xin, X., Li, L., Wang, Z., Zhang, Y., Li, J., Zhang, F., Wei, M., and Shi, X.: Global carbon budgets simulated by the Beijing Climate Center Climate System Model for the last century, Journal of Geophysical Research, 2013. 118, 4326-4347,, doi:10.1002/jgrd.50320, 2013.

Zeng, F.-W., Collatz, G., Pinzon, J., and Ivanoff, A.: Evaluating and Quantifying the Climate-Driven Interannual Variability in Global Inventory Modeling and Mapping Studies (GIMMS) Normalized Difference Vegetation Index at Global Scales, Remote Sensing, 5, 3918-3950; doi: 3910.3390/rs508918, 2013.

Zhu, Z., Bi, J., Pan, Y., Ganguly, S., Anav, A., Xu, L., Samanta, A., Piao, S., Nemani, R., and Myneni, R.: Global data sets of vegetation leaf area index (LAI)3g and fraction of photosynthetically active radiation (FPAR)3g derived from global inventory modeling and mapping studies (GIMMS) Normalized difference vegetation index (NDVI3g) for the period 1981 to 2011, Remote Sensing, 5, 927-948, 2013.

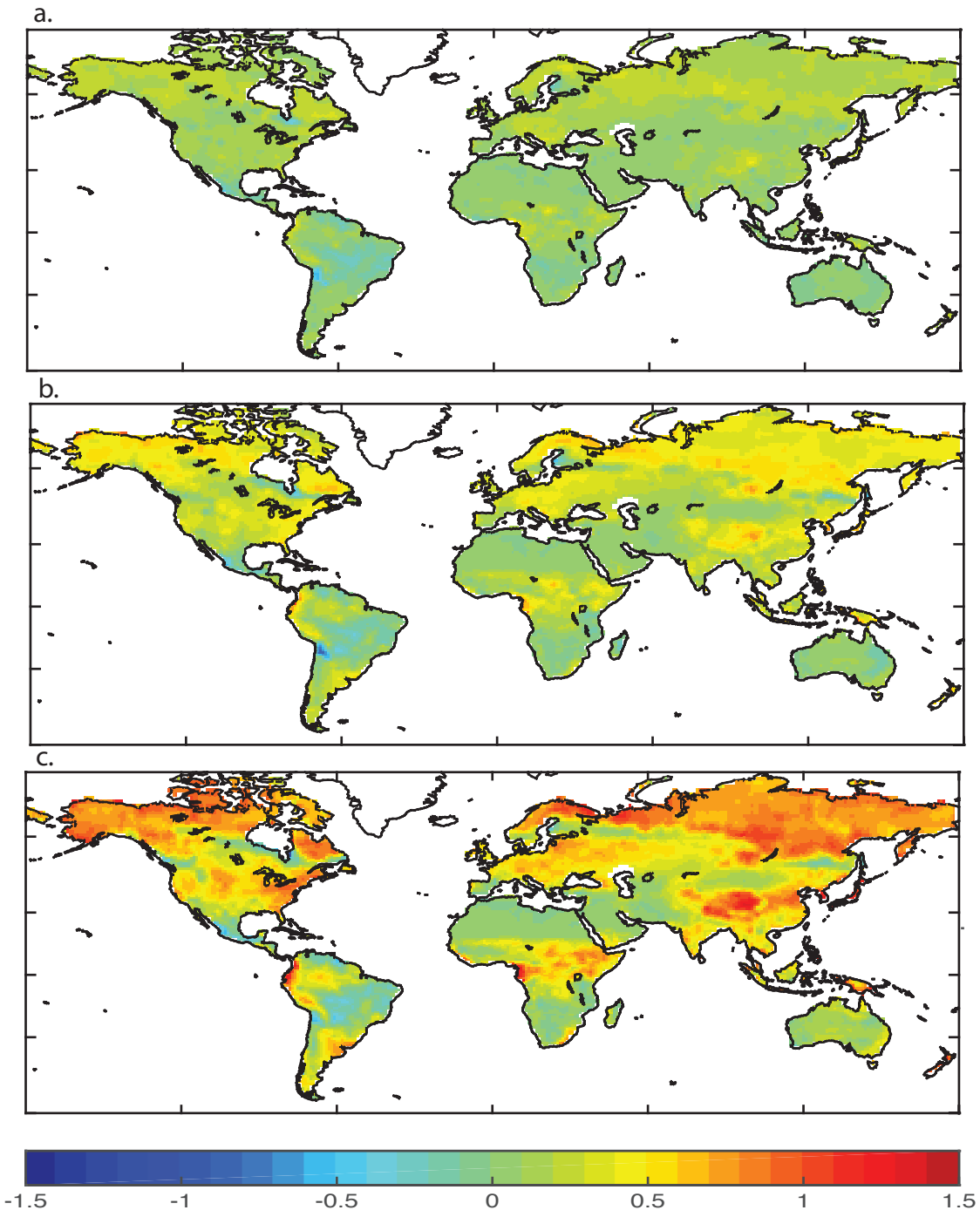
a.
b.
c.
-1.5
-1
-0.5
0
0.5
1
1.5

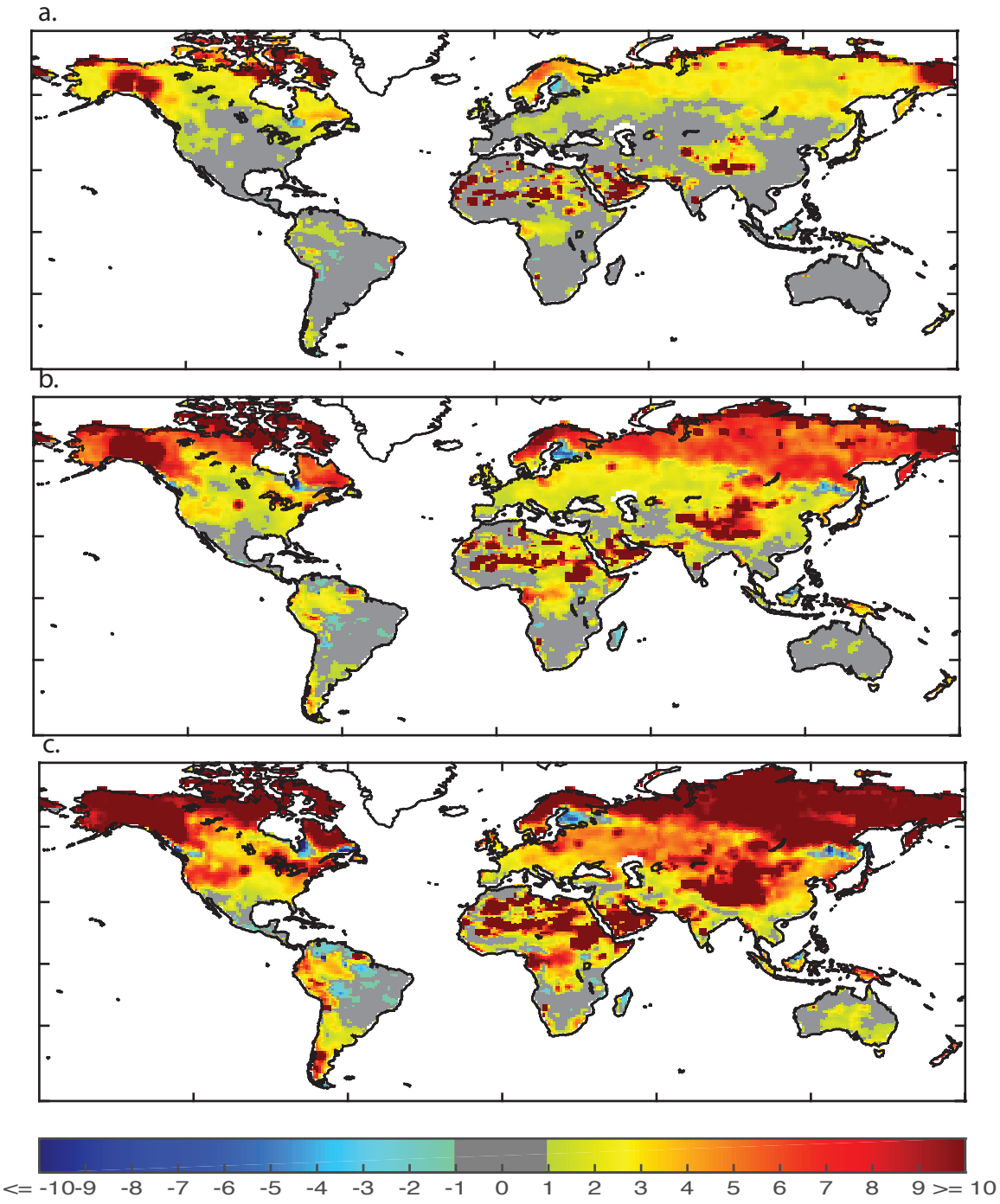
a.
b.
c.
<= -10 -9 -8 -7 -6 -5 -4 -3 -2 -1 0 1 2 3 4 5 6 7 8 9 >= 10

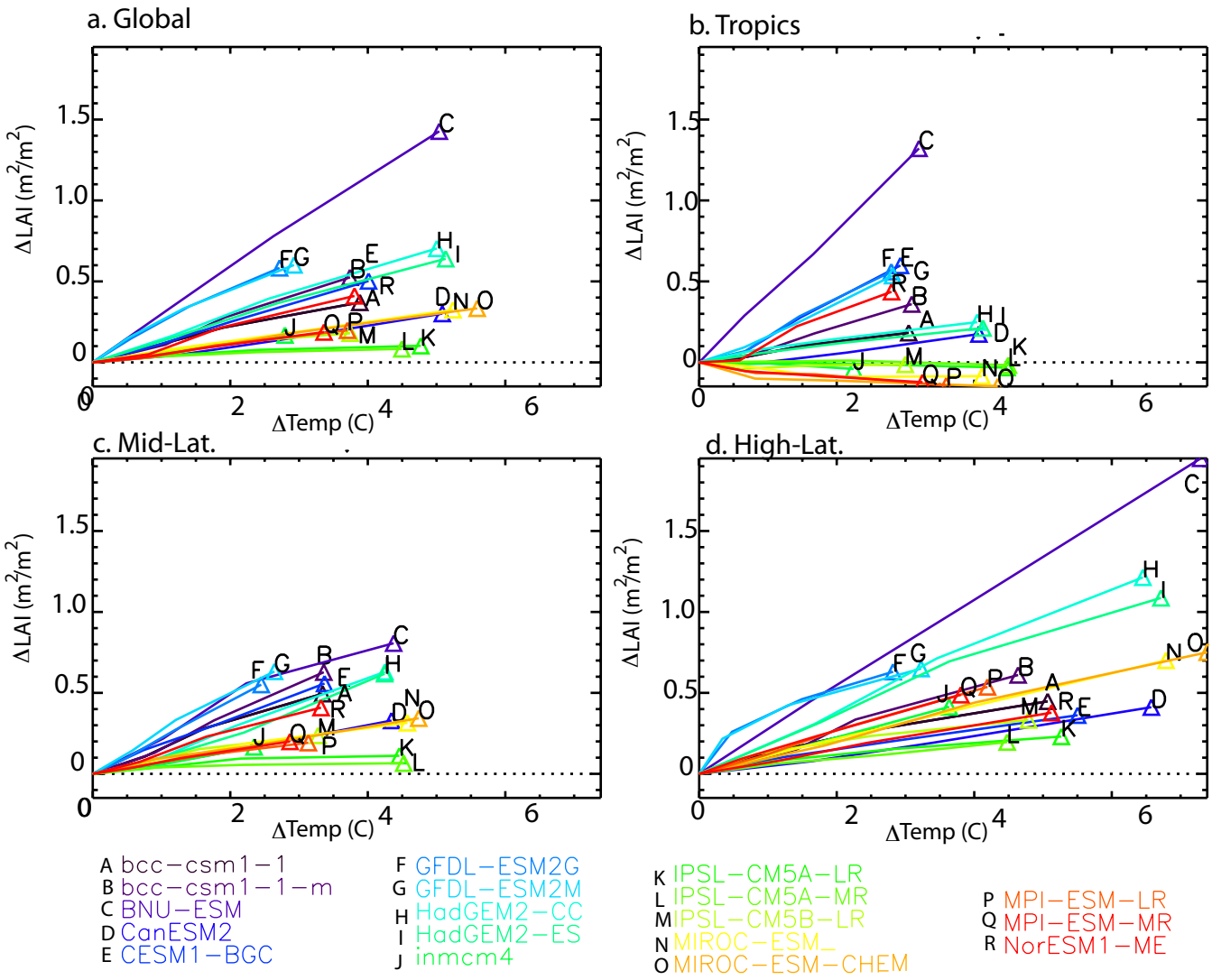
a. Global
b. Tropics
c. Mid-Lat.
d. High-Lat.
ΔLAI (m²/m²)
ΔTemp (C)
A bcc−csm1−1
B bcc−csm1−1−m
C BNU−ESM
D CanESM2
E CESM1−BGC
F GFDL−ESM2G
G GFDL−ESM2M
H HadGEM2−CC
I HadGEM2−ES
J inmcm4
K IPSL−CM5A−LR
L IPSL−CM5A−MR
M IPSL−CM5B−LR
N MIROC−ESM_
O MIROC−ESM−CHEM
P MPI−ESM−LR
Q MPI−ESM−MR
R NorESM1−ME

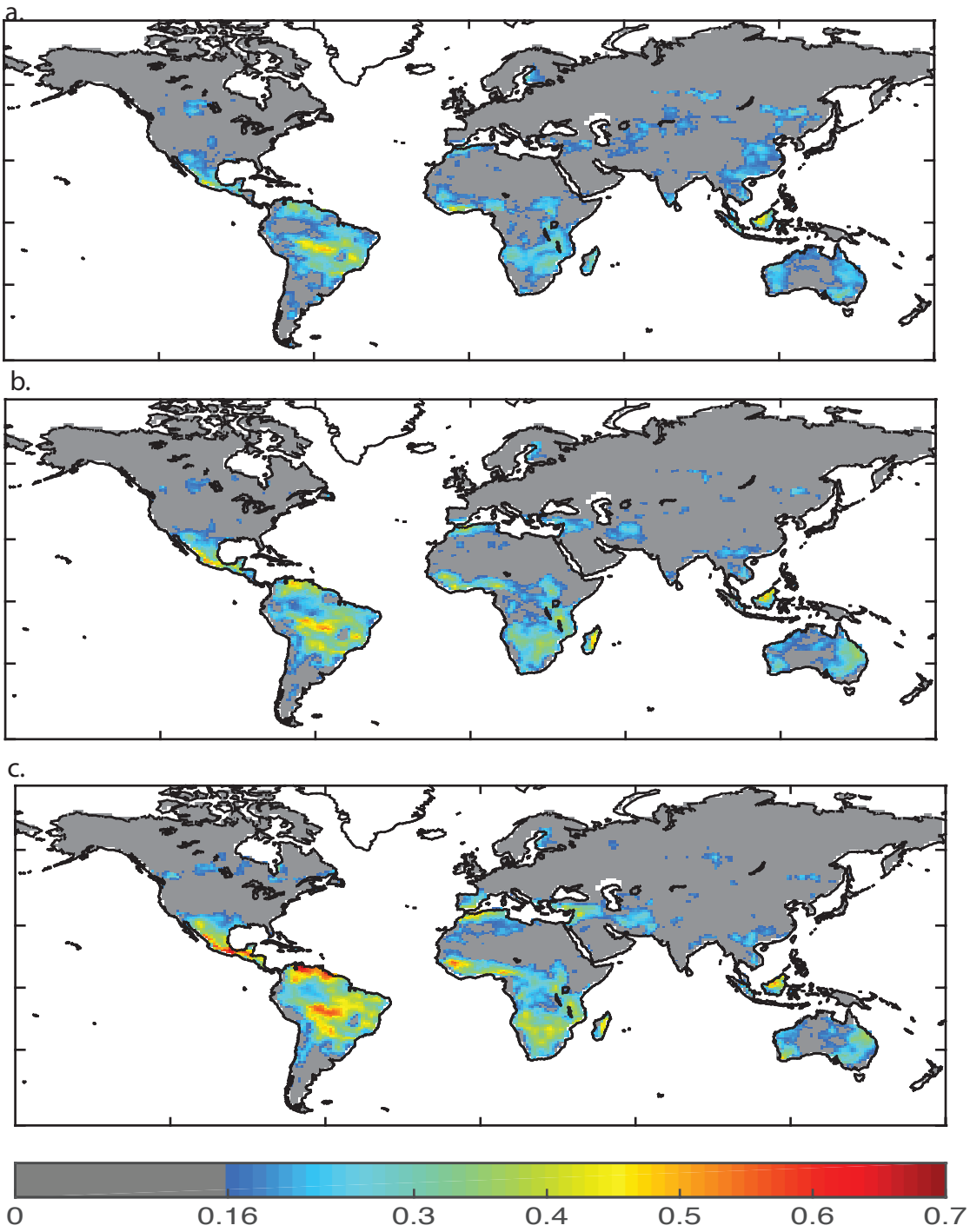
a.
b.
c.
0
0.16
0.3
0.4
0.5
0.6
0.7

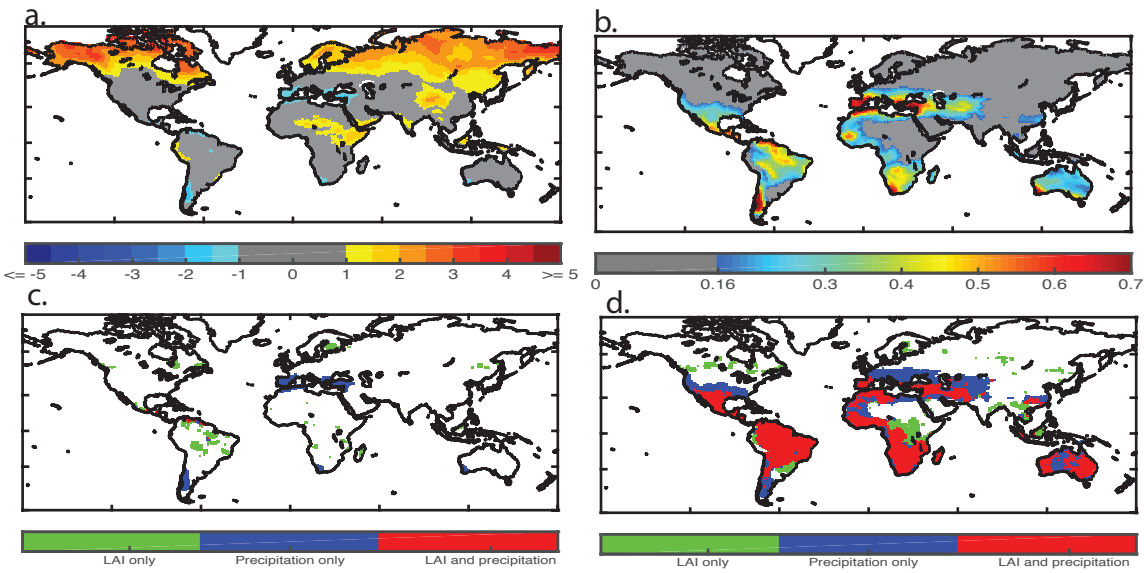
a.
<= -5
-4
-3
-2
-1
0
1
2
3
4
>= 5
b.
0
0.16
0.3
0.4
0.5
0.6
0.7
c.
LAI only
Precipitation only
LAI and precipitation
d.
LAI only
Precipitation only
LAI and precipitation

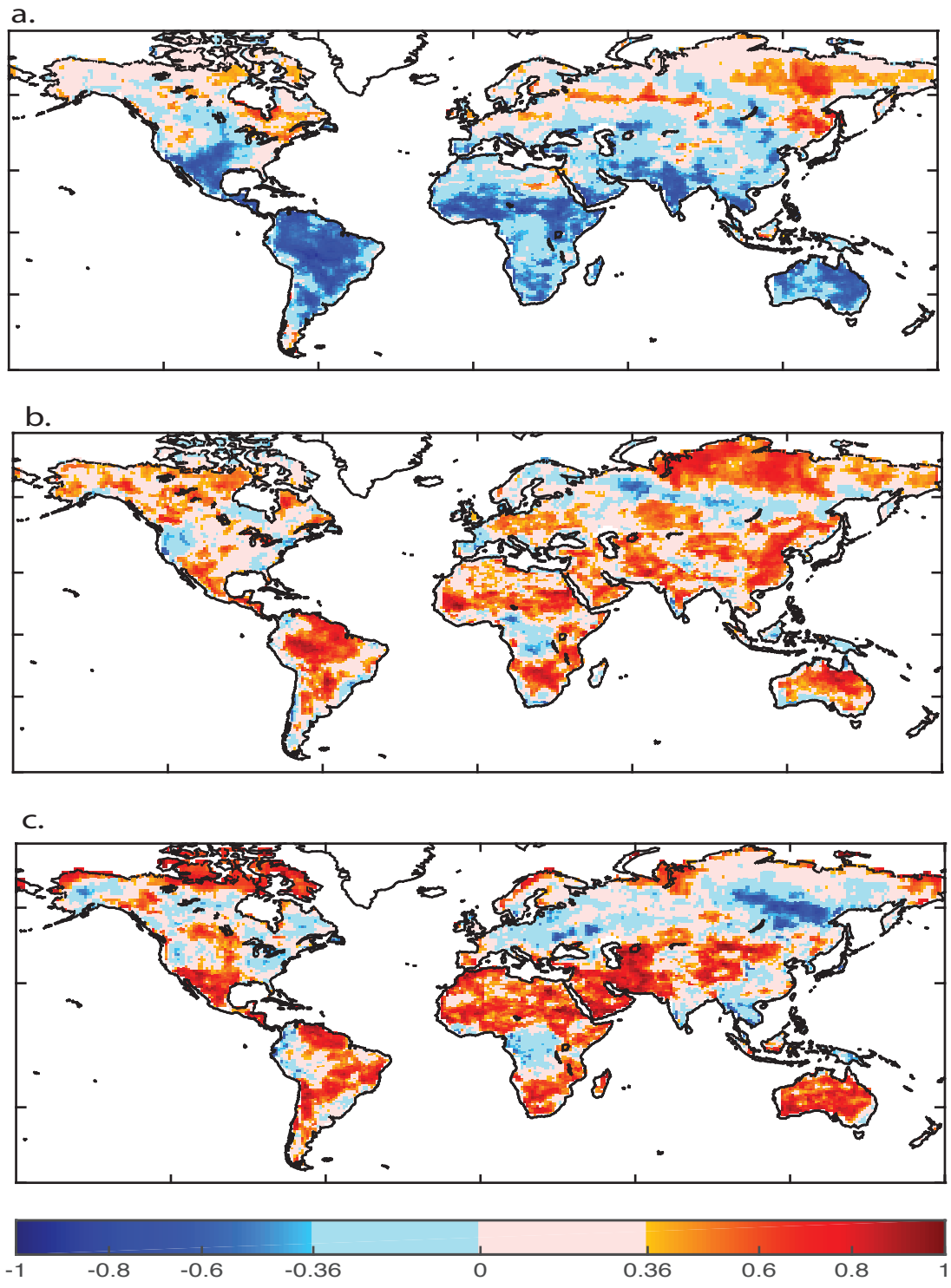
a.
b.
c.
-1
-0.8
-0.6
-0.36
0
0.36
0.6
0.8
1

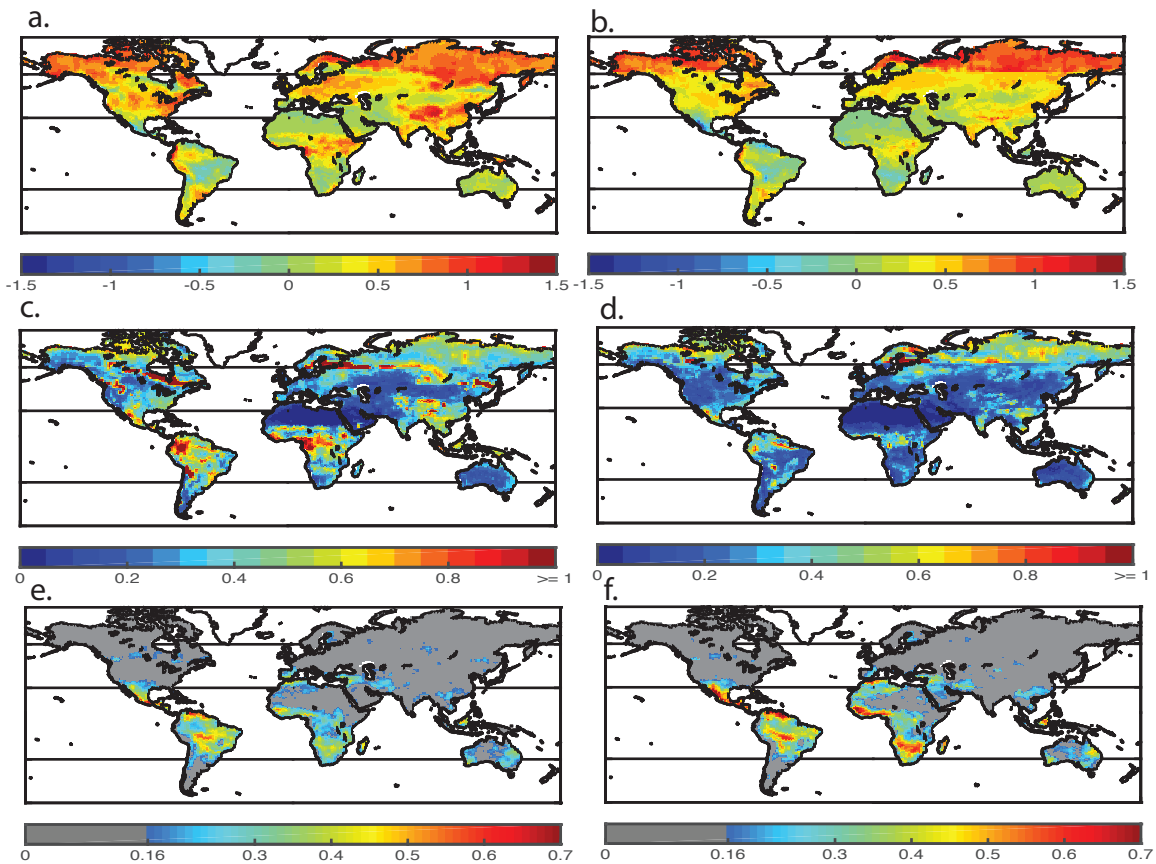
a.
b.
-1.5
-1
-0.5
0
0.5
1
1.5
c.
d.
0
0.2
0.4
0.6
0.8
>= 1
e.
f.
0
0.16
0.3
0.4
0.5
0.6
0.7

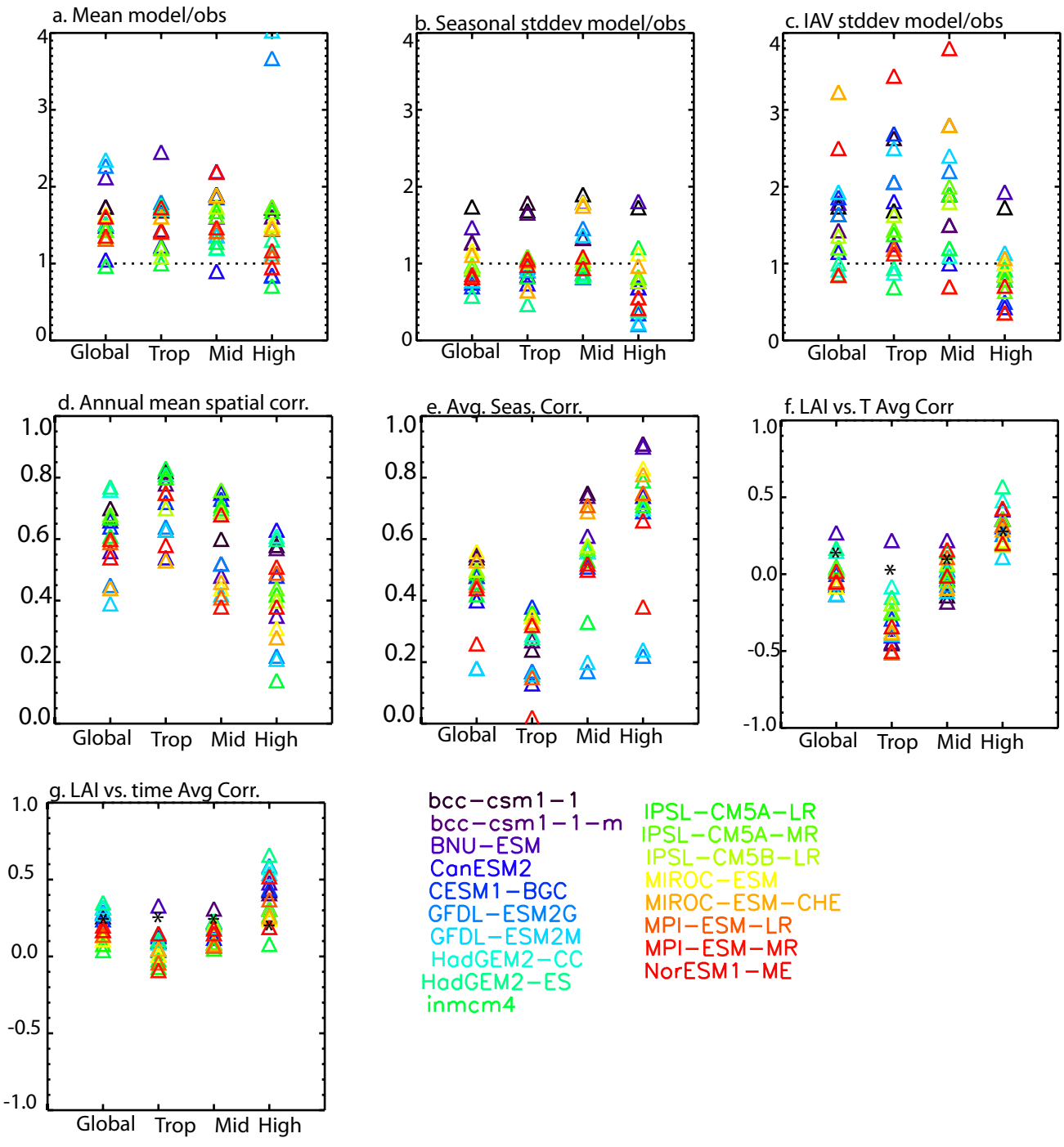
a. Mean model/obs
b. Seasonal stddev model/obs
c. IAV stddev model/obs
d. Annual mean spatial corr.
e. Avg. Seas. Corr.
f. LAI vs. T Avg Corr
g. LAI vs. time Avg Corr.
Global
Trop
Mid
High
bcc-csm1-1
bcc-csm1-1-m
BNU-ESM
CanESM2
CESM1-BGC
GFDL-ESM2G
GFDL-ESM2M
HadGEM2-CC
HadGEM2-ES
inmcm4
IPSL-CM5A-LR
IPSL-CM5A-MR
IPSL-CM5B-LR
MIROC-ESM
MIROC-ESM-CHE
MPI-ESM-LR
MPI-ESM-MR
NorESM1-ME

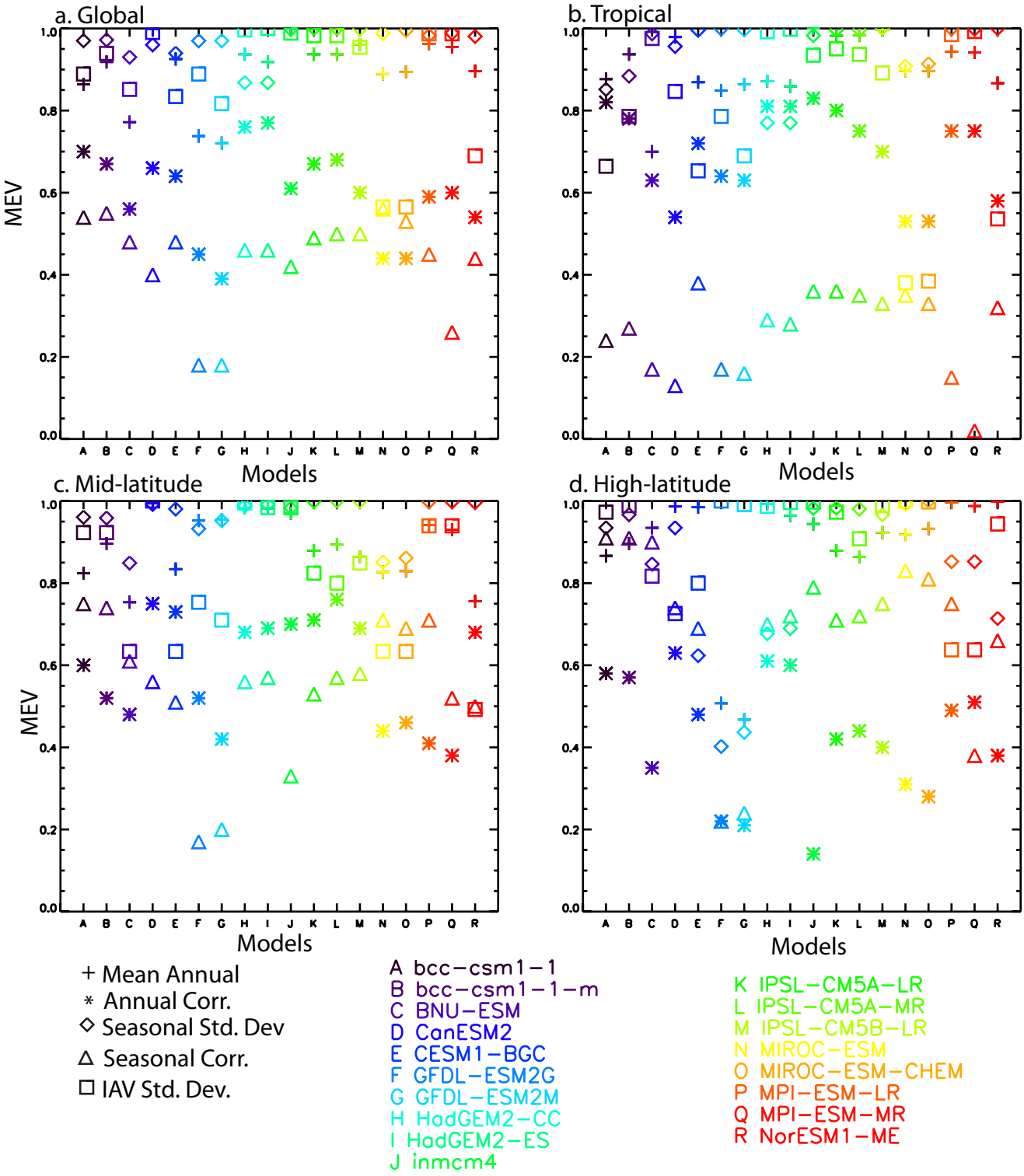
a. Global
b. Tropical
c. Mid-latitude
d. High-latitude
MEV
Models
A B C D E F G H I J K L M N O P Q R
0.0 0.2 0.4 0.6 0.8 1.0
+ Mean Annual
* Annual Corr.
◇ Seasonal Std. Dev
△ Seasonal Corr.
□ IAV Std. Dev.
A bcc-csm1-1
B bcc-csm1-1-m
C BNU-ESM
D CanESM2
E CESM1-BGC
F GFDL-ESM2G
G GFDL-ESM2M
H HadGEM2-CC
I HadGEM2-ES
J inmcm4
K IPSL-CM5A-LR
L IPSL-CM5A-MR
M IPSL-CM5B-LR
N MIROC-ESM
O MIROC-ESM-CHEM
P MPI-ESM-LR
Q MPI-ESM-MR
R NorESM1-ME

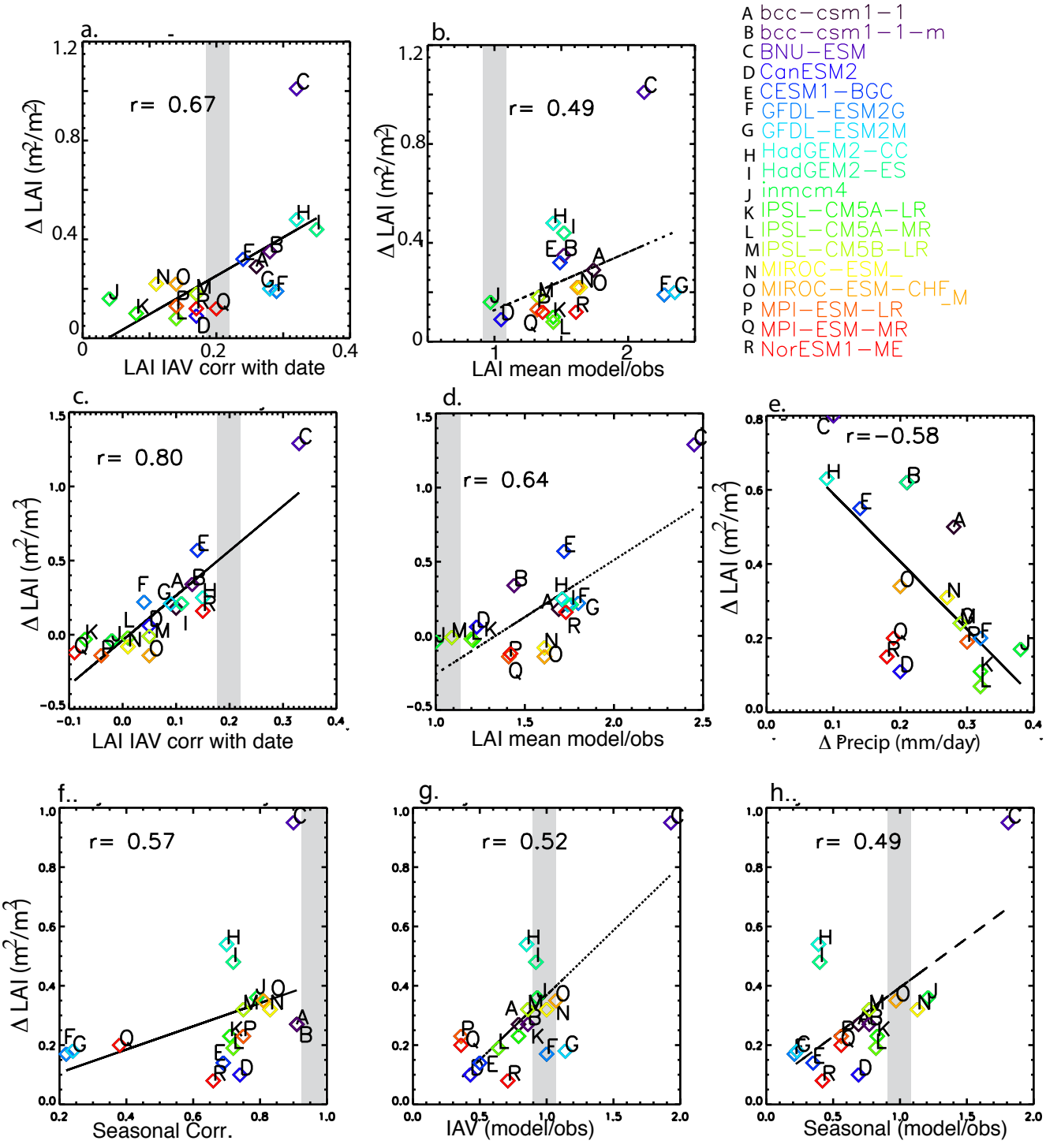
a.
r= 0.67
Δ LAI (m²/m²)
LAI IAV corr with date
b.
r= 0.49
LAI mean model/obs
A bcc−csm1−1
B bcc−csm1−1−m
C BNU−ESM
D CanESM2
E CESM1−BGC
F GFDL−ESM2G
G GFDL−ESM2M
H HadGEM2−CC
I HadGEM2−ES
J inmcm4
K IPSL−CM5A−LR
L IPSL−CM5A−MR
M IPSL−CM5B−LR
N MIROC−ESM_
O MIROC−ESM−CHF_M
P MPI−ESM−LR
Q MPI−ESM−MR
R NorESM1−ME
c.
r= 0.80
LAI IAV corr with date
d.
r= 0.64
LAI mean model/obs
e.
r=−0.58
Δ Precip (mm/day)
f..
r= 0.57
Seasonal Corr.
g.
r= 0.52
IAV (model/obs)
h..
r= 0.49
Seasonal (model/obs)